CZECH TECHNICAL UNIVERSITY IN PRAGUE
Faculty of Civil Engineering
Thákurova 7, 166 29 Prague 6, Czech Republic

MASTER'S THESIS PROPOSAL

study programme: Civil Engineering

study branch: Advanced Masters in Structural Analysis of Monuments and Historical Constructions

academic year: 2017/2018

Student's name and surname: Nigar Shaikh

Department: Department of Mechanics

Thesis supervisor: Ing. Jan Válek, PhD.

Thesis title: Characterisation of historic burnt clay building ceramics with respect to their production technology and raw material provenance

Thesis title in English see above

Framework content:

Provide characteristics of a burnt clay of a local provenance and compare them with the historic floor tiles used in the church of st. Jan of Nepomuk (UNESCO protected site).

Assignment date: 9/04/2018 Submission date: 02/07/2018

If the student fails to submit the Master's thesis on time, they are obliged to justify this fact in advance in writing, if this request (submitted through the Student Registrar) is granted by the Dean, the Dean will assign the student a substitute date for holding the final graduation examination (2 attempts for FGE remain). If this fact is not appropriately excused or if the request is not granted by the Dean, the Dean will assign the student a date for retaking the final graduation examination, FGE can be retaken only once. (Study and Examination Code, Art 22, Par 3, 4.)

The student takes notice of the obligation of working out the Master's thesis on their own, without any outside help, except for consultation. The list of references, other sources and names of consultants must be included in the Master's thesis.

....
Master's thesis supervisor Head of department

Date of Master's thesis proposal take over: July 2018

.....
Student

This form must be completed in 3 copies – 1x department, 1x student, 1x Student Registrar (sent by department)

No later than by the end of the 2nd week of instruction in the semester, the department shall send one copy of BT Proposal to the Student Registrar and enter data into the faculty information system KOS.

(Dean’s Instruction for Implementation of Study Programmes and FGE at FCE CTU Art. 5, Par. 7)

DECLARATION

Name:	Nigar Shaikh
Email:	nigar21093shaikh56@gmail.com
	ni21093@yahoo.com

Title of the Msc Dissertation:	Characterization of historic burnt clay building ceramics with respect to their production technology and raw material provenance
Supervisor(s):	Ing. Jan Válek, PhD.
Year:	2017/2018

I hereby declare that all information in this document has been obtained and presented in accordance with academic rules and ethical conduct. I also declare that, as required by these rules and conduct, I have fully cited and referenced all material and results that are not original to this work.

I hereby declare that the MSc Consortium responsible for the Advanced Masters in Structural Analysis of Monuments and Historical Constructions is allowed to store and make available electronically the present MSc Dissertation.

University:	Czech Technical University, Prague
Date:	2nd July 2018
Signature:	_____

This work is dedicated to my parents and my deceased classmate and friend Hely.

ACKNOWLEDGEMENTS

First of all I would like to acknowledge consortium coordinator, Prof. Paulo Lourenco (University of Minho) and entire SAHC team, for providing me this opportunity to explore field of structural analysis of historic buildings. I would also like to thank Prof. Petr Kabele (Czech technical University) for the thesis topics and providing necessary institutional support.

I am very grateful to my supervisor Prof. Jan Valek for giving right directions, shaping and formulating my thoughts and understandings about the topic. I was humbled to be working on this thesis as a part of Institute of Theoretical and Applied Mechanics (ITAM).

I was privileged to carry out my tests at Centre of Excellence, Telč, under the supervision of Alberto Viani and directions from Konstantinos Sotiriadis

I thank Olga Skružná and RNDr. Petr Kozlovcev for their cooperation and help throughout the thesis.

I am thankful to the staff and technicians of Czech Technical University, ITAM and Centre of Excellence who aided and co-operated in every way possible.

This work wouldn't have been possible without my family and friends, who stood beside me throughout my study.

Lastly I would like to thank Jae Kang for always encouraging me and providing moral support, and all the "Real Prague boys" for creating a home away from home.

ABSTRACT

Bricks, tiles and other burnt clay building materials have been used as construction material since antiquity. Their mineralogical composition and physical properties are mainly affected by the burning conditions and temperature and the raw clay composition. The characterization of the burnt clay units can lead to valuable information about the historic production technologies and material sources. The aim of this project was to characterize the burnt clay specimens, prepared from local raw material sources, in order to understand the burning temperature and production process of the historic flooring tiles used in the church of St. John of Nepomuk (cultural heritage national monument and UNESCO protected site). Thus the original burnt clay tiles can be replicated and the flooring can be restored using the tiles prepared from the formerly used raw material and technology. This experimental study focused on understanding the mineralogy and composition of specimens from particularly selected raw clays burnt at different temperatures. The study was achieved by performing X-ray diffraction, thermal analysis, optical microscopy and mechanical tests. The results of the burnt specimens were discussed in comparison with the original tile properties. The research work led to the description of the behaviour and characterization of the ceramic units made from the local clays burnt at temperatures from 650 °C to 1050 °C.

Key words: burnt clay ceramic tiles, Zelená Hora, mineralogy, firing temperature, XRD-QPA, raw material composition

ABSTRAKT

Materiálové zhodnocení historické pálené stavební keramiky s ohledem na výrobu a surovinovou provenienci

Cihly, dlaždice a další materiály z pálené keramiky jsou jako stavební materiály používány od starověku. Jejich mineralogické složení a fyzikální vlastnosti jsou ovlivněny zejména teplotou a podmínkami výpalu a složením suroviny. Analytický materiálový průzkum stavebních dílů z pálené hlíny může vést k cenným informacím o historických výrobních technologiích a surovinových zdrojích. Cílem tohoto projektu bylo charakterizovat vzorky pálené hlíny připravené z místních surovin za účelem lepšího porozumění vlivu teploty výpalu a výrobního procesu na historické podlahové dlaždice použité v kostele sv. Jana Nepomuckého (národní památka kulturního dědictví a místo chráněné organizací UNESCO). Původní keramické dlaždice by tudíž bylo možné replikovat a podlahu tak restaurovat pomocí dlaždic připravených na základě původně použitých surovin a technologií. Tato výzkumná studie se zaměřila na porozumění mineralogie a složení vzorků z vybraných cihlářských surovin vypálených při různých teplotách. Studium bylo dosaženo provedením rentgenové difrakce, tepelné analýzy, optické mikroskopie a mechanických testů. Výsledky vypálených vzorků byly diskutovány ve srovnání s vlastnostmi původních dlaždic. Výzkumná práce vedla k popisu chování a charakterizaci keramických prvků z místních jílů pálených za teplot od 650 °C do 1050 °C.

Klíčová slova: pálená stavební keramika, Zelená Hora, mineralogie, teplota výpalu, XRD-QPA, složení surovin

Table of Contents

LIST OF FIGURES

LIST OF TABLES

1. INTRODUCTION

The Czech Republic located in the central region of Europe, is known for its remarkable historic sites and rich culture. In total UNESCO has 12 sites listed as World Heritage in the Czech Republic (UNESCO, 1994) and is working in the benefit of these sites. Many projects are under pipeline for the conservation of these World Heritage sites. A lot of efforts pertaining to research have to be undertaken for the restoration plan of the historic sites. The materials used for repair and reconstruction must be compatible with the original material used in construction of these structures.

1.1 Research Aim

This research is based on a practical conservation project that is pertains to restoration of the ground tile flooring of the church of St. John of Nepomuk which is listed as World Heritage site by UNESCO. The pilgrimage church of St. John of Nepomuk at Zelená hora (Figure 1) is an important cultural heritage monument and any intervention should be carefully considered. The current conservation plan examines restoration of the original ground floor tiles including a reconstruction of previously lost parts. (Mojmir Horyna, 2008) The reconstruction should be based on the original material and technologies. In order to contribute to the evaluation of this reconstruction this research project has been carried out with the following goals

- Sample local clay resources in the vicinity of the church
- Evaluate behaviour of the local clay samples burnt at different temperatures

This work is aimed at providing material characteristics that can contribute to the understanding of the local clay resources potentially suitable for the tile replicas production. It also aimed to contribute to the discussion about the material origin of the historic tiles. In addition the effects of the burning temperatures on the material performance were assessed.

Figure 1- Location of the pilgrimage church of St. John of Nepomuk in Czech Republic. (space, 2017), (Dijk, 2017)

2. LITERATURE REVIEW

The constituents of burnt clay ceramics, production and the analytical methods which can be employed on the units are discussed in nutshell in this part.

2.1 Burnt ceramic units

Burnt ceramic units are one of the oldest and most commonly used construction materials. Apart from their use in structural elements like foundation and walls, they were widely used for roofing and flooring of historic structures, decorative cladding etc. Clay is the basic raw material used for brick and burnt ceramic production. Manufacturing process of bricks includes grinding, sieving, mixing with water, moulding and firing the brick units. The firing temperature generally ranges from 600-1100 °C (K Ambrose, 2001). The different clay minerals are categorized in the Figure 2. During the course of firing, clay minerals like illite-chlorite, quartz, calcite and dolomite, sodium and potassium feldspars undergo some characteristic reactions, redefining the mineralogical composition and microstructure (Alberto Viani, 2016). Present time demands conservation of historic materials and replacement with the compatible material. The characterization of the old bricks and assessment of the firing conditions applying thermo analytical criteria can lead to reconstruction of former production conditions and compatible material for future use (A. Moropoulou, 1995).

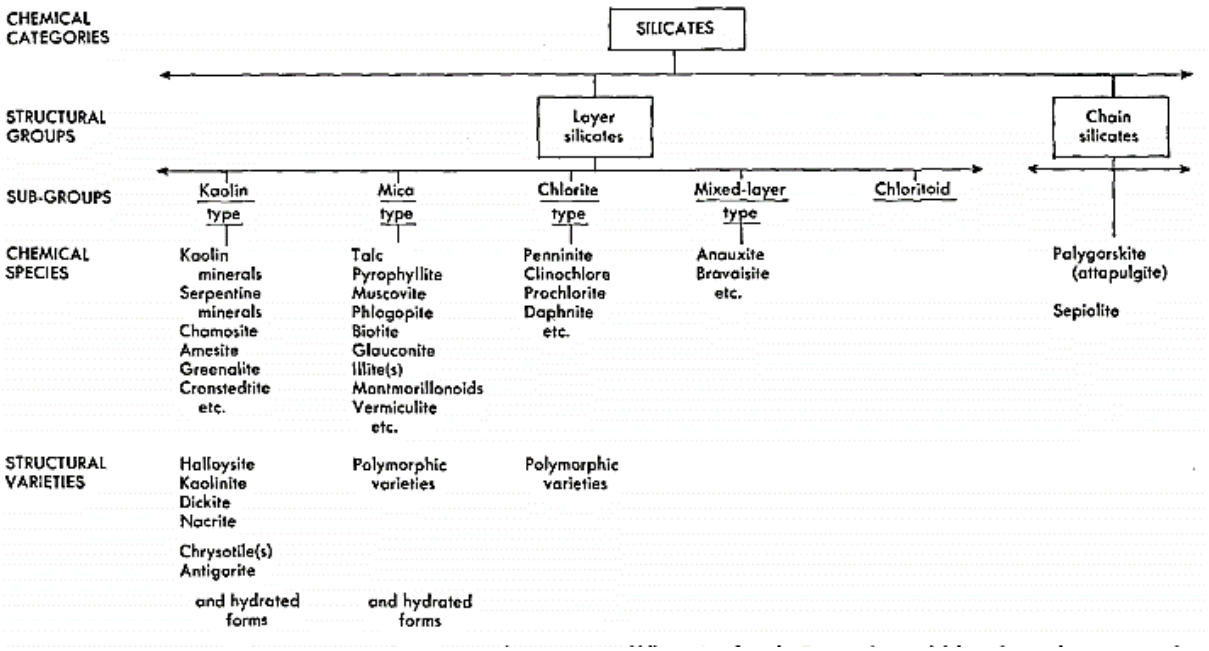

Figure 2- Clay mineral categories. (Brindley)

2.2 Analytical methods

Analytical methods can help in evaluating the durability and mechanical performance of burnt clay units and thus identifying their compatibility with other historic building materials. In general to characterise historic burnt clay units it has been recommended to integrate information from different analytical techniques and adopt combinations of different methods. Following section describes analytical methods based on published literature that were considered to be applied for characterization of burnt clay units.

2.2.1 Open porosity, Water absorption, Specific density and Interconnectivity of pores

The pore distribution and interconnectivity of pores are important for determining the durability against weather conditions and salt attack resistance of the burnt ceramic units (Johnson, 1940). The open pores (also cracks) facilitate fluid movement within the material structure and also relate to the strength of the unit. Apart from this porosity can be a significant parameter in determining the firing temperature of the ceramic units. Firing of clay units and duration of firing, produces a series of mineralogical, textural, and physical changes that depend on many factors and influence porosity. As deduced by Giuseppe Cultrone, substantial variations in the composition and/or concentration of mineral phases cause changes in the pore system. For instance, when the raw material contain calcium or magnesium carbonate than its decomposition and the release of CO_2 leads production of porous ceramics at temperatures above app. 900 °C (Giuseppe Cultrone *. E., 2004). The temperature changes during firing leads to expansion and contraction of clay minerals which produce exothermic and endothermic reactions. These reactions can be determined and verified by thermal analysis. The determination of microstructure and pore size can also contribute to the correlation of the production process and the firing temperature. Porosity (Apparent porosity, Bulk density and Total porosity) can be measured using the Archimedes buoyancy technique with dry weights, saturated weights and immersed weights in water (Berger, 2010). X explains the principle for understanding open and closed pores.

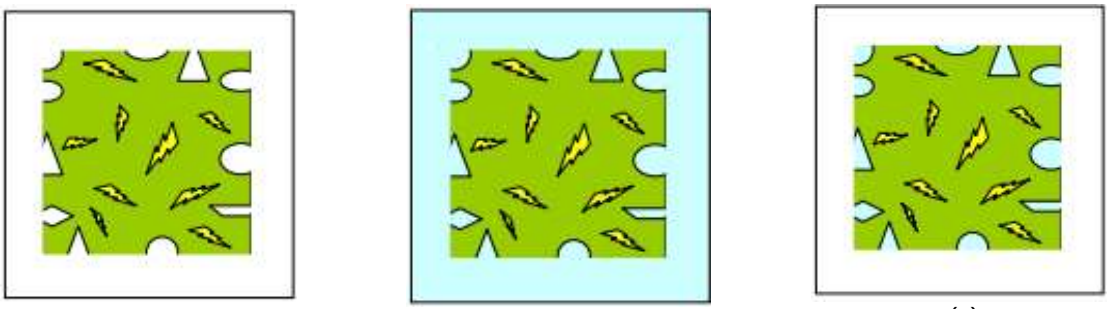

Figure 3- Green part is the solid material, yellow part depicts closed pores and white shapes illustrates open pores; (a) solid body; (b) suspended body; (c) soaked body (Berger, 2010)

The degree of pore interconnectivity can be obtained from forced and free water absorption %. It can be used as a function of total porosity.

2.2.2 Flexural and compressive strength test

The mechanical properties of the burnt ceramic units can be identified by flexural and compressive testing. These tests can provide information regarding the bearing capacity of the bricks, thus aiding the characterization of the bricks. The bearing capacity of the original tiles can be kept as benchmark while producing new tiles for restoration work. The flexural strength is determined by performing three point bending test as Euro code EN 1052-2:1999. The Figure 4 below shows the schematic of a three point bending test.

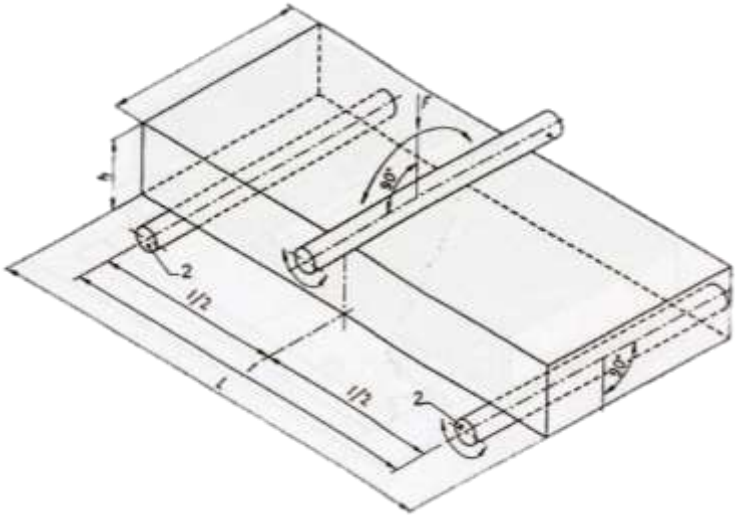

Figure 4- A schematic of three point bending test.

2.2.3 X-ray diffraction

X-ray diffraction is one of the most effective analytical methods employed to determine the mineralogy of brick. X-ray diffraction is also used for phase quantification in the material. The underlining principle is to obtain patterns diffracted from different plans of atom. A typical diffraction spectrum consists of a plot of reflected intensities versus the detector angle 2-THETA or THETA depending on the goniometer configuration (ThermoARL, 1999). This spectrum when plotted for bricks or burnt ceramics fired at different temperature, can be used to detect the phase changes in the mineralogy of the specimen. Using software like TOPAS 4.2 (Bruker AXS) one can identify the minerals present and their quantity in the specimen. The Quartz-Feldspar quantity, Ca-rich unit, Ca-poor unit, minerals forming at high temperatures, minerals disappearing at high temperatures can be identified using the results from the X-ray diffraction analysis. As per the experimental procedures if the material to be tested is suspected of containing amorphous fraction then it should be spiked with a known amount of internal standard (corundum, silicon, fluorite, rutile and zincite) (Alberto Viani, 2016). The amorphous content can be obtained using the spectrum generated by the software. Thus the mineralogical characterization of the brick specimen can be accurately carried out by X-ray diffraction and Quantitative phase analysis (QPA).

2.2.4 Thermal Analysis

The characterization of historic ceramics can be improved by thermal analysis. Thermogravimetric analysis (TG) provides the weight loss with temperature, identifying the prominent phase changes. Derivative thermal analysis (DTA) curves can be used to detect the exothermic and endothermic peaks which is representative of formation/transformation of minerals. Therefore the main successive phases associated with the dehydration and thermo-oxidative degradation can be investigated using thermal analysis (Földvári, 2011). The dehydroxylation, decomposition and transformation phases can be identified and used for the characterisation of former production conditions as well as estimating the firing temperature of the historic material. The thermal behaviour of materials like bricks is coherent with their chemical and mineralogical composition (Fierascu, 2009). Hence the results obtained from the Derivative thermal analysis (DTA) and Thermogravimetric analysis (TA) can be correlated with mineralogy derived by X-ray diffraction. This allows to verify mineralogical change and phase transformations occurring in the brick structure at different temperatures. Fierascu even stated that if applied correctly Thermogravimetric analysis (TG) and DTA can an indispensable tool in discovering special technological features associated with brick.

2.2.5 Optical Microscopy

The composition and microstructure of the burnt ceramic can be observed closely using an Optical Microscope. Optical Microscopy provides information at a qualitative level. Inclusions can be examined to determine mineral (or rock fragment) identity, grain size (using the Wentworth grain size scale), grain shape, and volume percentage composition using standard petrographic techniques and comparative charts (Ruth Ann Armitage a, 2006). The dominant minerals can be identified using petrographic analysis. The pore and interconnectivity of the pores can be qualitatively analysed. Minerals appearing, transforming and disappearing with different firing conditions can be distinguished. Colour change, grain shape-size, cracks etc. can be quantified using optical microscopy. The polarized optical microscope helps in differentiating feldspar and quartz grains along with the pores present in the specimen. The observations from optical microscopy can be combined with X-ray diffraction results and interpreted to obtain more quantitative results.

2.3 Case study

As discussed in Chapter 1, the case study for research is one of the UNESCO listed structure of Czech Republic. Thus the understanding about the structure, its design, material and previous intervention on it are important factors which are highlighted in this section.

2.3.1 The Church of St. John of Nepomuk

The pilgrim church dedicated to St. John of Nepomuk, is located at Zelená hora, at the edge of Žďár nad Sázavou, Czech Republic, near the historical border between Moravia and Bohemia as shown in the Figure 1.

It was built during 1719 to 1722 AD by the Prague Bohemian architect Jan Blažej Santini Aichel under the influence of Václav Vejmluva, abbot of the Cistercian monastery in Žďár. Abbot Václav Vejmluva was admirer and devotee of John of Nepomuk. Soon after the miraculous discovery of the saint's torn tongue in 1719, the abbot declared the construction of the shrine and presented the design idea of a new pilgrimage church to Jan Santini (Růžička, 2014).

The ambits to shelter the pilgrims were constructed in 1730 after the death of the architect (Růžička, 2014). The church is well known for its architectural and symbolic interpretations.

The entire complex consists of the main church and the five pilgrim ambits with chapels surrounding the church (Figure 5). The complex was inscribed in the Register of World Cultural and Natural Heritage of UNESCO in 1994.

(a) (b)

Figure 5- (a) Bird view of the St. John of Nepomuk; (b) One of the five chapels surrounding the main church. (Zamekzdar, n.d.) (Fuxa, n.d.)

2.3.2 The design of the Church

The architect Jan Santini used the abbot´s idea of the church constituting the main role played by the pattern of a star, into an extraordinarily impressive form which broke the stereotype design and forms of the churches during that time period. A lot of emphasis was laid on creating more open space.

The construction of the first two towers of the ambit besides the western entrance was completed by 1730. The archives from 1735 claim that the final fifth ambit was unfinished until then.

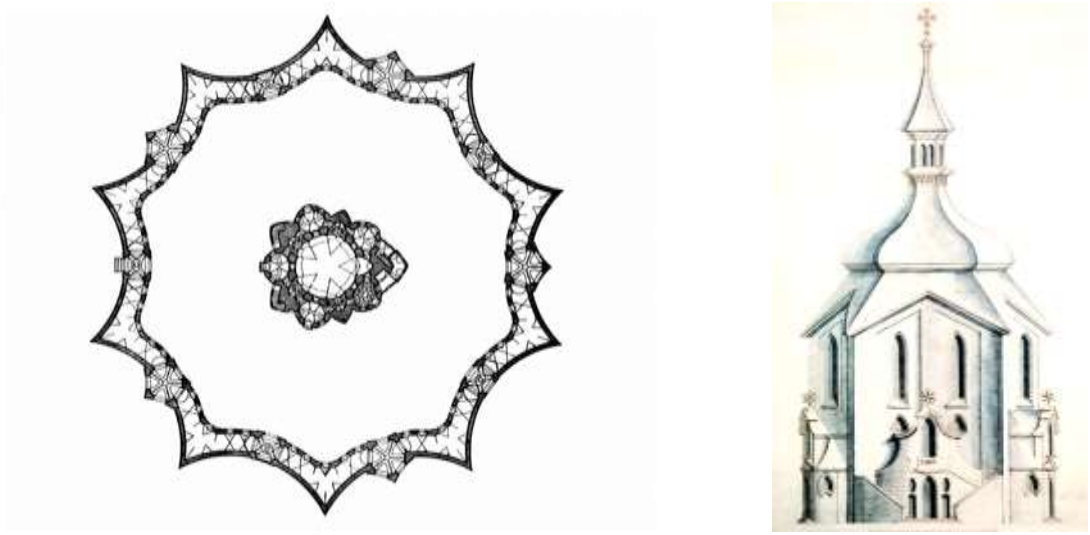

(a) (b)

Figure 6- (a) Plan of the church and its ambit with chapels; (b) Elevation of the main church. (Church of St. John of Nepomuk, 2016)

2.4 Analysis of the Floor

2.4.1 Floor tiles

The main interest of this work is in the ground floor but the same tiles that were originally used in the ground floor were also used in the first and second galleries. Sample of original tiles is shown in Figure 7. The original written sources mentioning the floor or stating its condition are very few.

Figure 7- Illustrations of floor tiles used in the ground and first floor of the church.

In the inventory from 1824 there is stated that the ground floor is tiled partially with stone and partially with deliberately shaped bricks (Chudárek, Z, 2009).

During the repair works between 2001 and 2003 the floors were documented and some conservation interventions were carried out.

2.4.2 Design and state of the original ground floor tiles

The original floor was laid with a combination of pentagonal and diamond tiles. The design created a pattern of five-pointed stars as shown on the Figure 8. The side chapels consist of oblong tiles. The diamond tile was laid in between these five tiles as shown in Figure 9.

Figure 8- The formation obtained as a result of arrangement of the tiles for the ground floor.

These formations of the tiles evoked the illusion of special structure when viewed from top. Observing the partially preserved tiles Chudarek (2009) judged that the tiles were of black, red and white (yellow) colour and he also suggested how the original floor should had looked like.

Figure 9- Combination of pentagonal and diamond tiles.

This floor was damaged due to the long-term leakage through the roof that was destroyed in the fire of 1784. Damaged tiles were replaced with marble tiles (36×36 cm) which were of smaller dimensions compared to the tiles used in the central nave (Figure 10).

Figure 10- Replaced marble tiles of 36×36 cm dimension.

These repairs were executed in the areas between the entrance and the hatch of the crypt. Few tiles were replaced in the middle part of the nave of the church and the presbytery using old square marble tiles of dimension 45×45 cm. This created complications which included change in the direction of the tiles, irregular joints and ceramic-marble combinations aesthetically not fitting to the original design that followed and emphasized the central space of the church.

Figure 11- Central space of church with marble tiles of 45×45 cm dimension.

The hall near the eastern staircase was intervened using bricks for pavement. The tiled floor was recently repaired in 2002 to 2003. The repair was planned in two phases. The first phase dealt with the defects that were affecting the safety of visitors and those that caused further damage to the original tiles. The second phase involved a gradual rehabilitation of the original floor of the church. The second phase has not been implemented yet. Observing the present state of the ground floor, the weathered tiles and marble tile interventions are noticeable. The tiles have been damaged near corners of the church. In areas of heavy foot traffic the abrasive effect is prominent. Different shades of colours are visible, due to fading effect (Figure 12).

Figure 12- Lighter shade of tiles observed cause by heavy traffic and abrasion.

The original tiles were subjected to material analysis during the first repair phase leading to a surprising results suggesting that the material was “artificial stone” i.e. local aggregate bonded with unknown binder (probably water glass) (Chudárek 2009), L. Kryl, Žďár nad Sázavou – Poutní kostel sv. Jana Nepomuckého, technologický průzkum vzorků dlažby, 2002). Based on this finding cement based binder with aggregate and pigments was used to carry out local repairs and produce copies.

`

3. METHODOLGY

To achieve the research goals a systematic methodology was adopted. The following chart shows the steps of the approach undertaken for this research:

Table 1- Study approach undertaken for the project.

Sample preparation	• Selection of location for raw clay sample ➢ Studying the locations of probable clay pits and brick kilns during the era of construction of the church and retrieving raw clay samples to be tested.
	• Preparation of specimens from raw clay ➢ Mixing and moulding the raw clays to prepare specimens. Firing these raw clay specimens at different temperatures.
Tests and methods	• Procedure of analytical tests performed ➢ Details of tests like open porosity, water absorption, flexural and compressive strength, X-ray diffraction, thermal analysis and optical microscopy.
Results	• Results from analytical tests
Discussion	• Derivation from results ➢ Comparison and correlation of results from different tests.
Conclusion	• Final remark after analysis of the results

4. SAMPLE PREPARATION

In order reproduce the tiles for repair/reconstruction works, it is necessary to use identical raw material and production technique. This section elaborates the details of selecting the site for collection of raw clays, mixing process for the raw clay samples collected, moulding and firing process of the moulded specimens.

4.1 Raw clay collection

The task was to locate the position of clay pits that were potentially in operation during the era of construction of the Pilgrim church of St. John Nepomuk. The idea was to collect samples of raw clay and compare it with the material of the original tiles. To identify the clay pits 1st and 2nd Military Survey maps were studied along with the Cadastral maps from the first half of the 19th century. The oldest maps of the 1st Military Survey come from the second half of the 18th century (1764-1768) and show the situation approximately 50 years after the church was founded. Three potentially relevant sites were identified as shown in the map below (Figure 13, 14 & 15).

A - Světnov – 4.4 km north from the church, clay pit and brick production existed in the 18th century (1st MS)

B - Kamenný rybník (Stone pond) – 3.8 km south of the church, clay pit only (Cadastral map)

C - Cihelna (Brick kiln, Z.O. on the map) – 3.0 km south of the church, clay pit and kiln (Cadastral map).

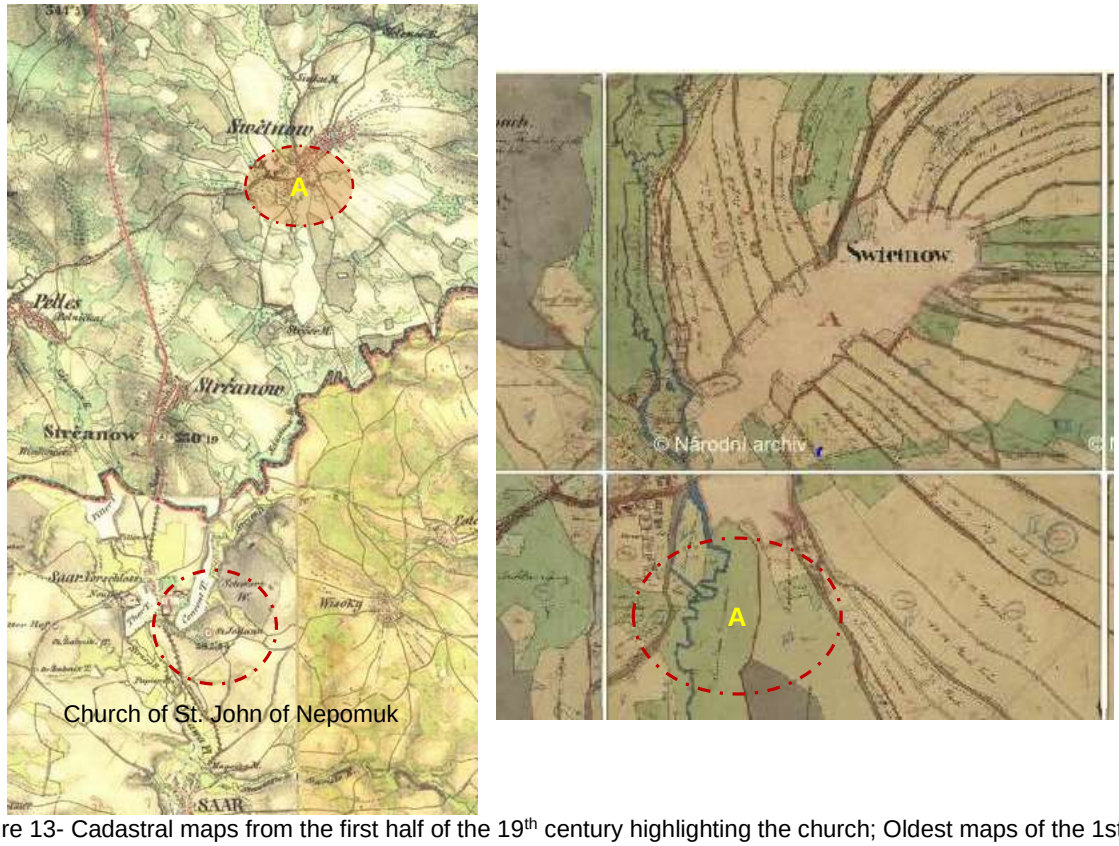

Figure 13- Cadastral maps from the first half of the 19th century highlighting the church; Oldest maps of the 1st Military Survey come from the second half of the 18th century showing location of site “A”. (Geoinformation, n.d.) (Stabilní katastr Čech - Světnov, původně Swietnow, n.d.)

The X map is the 18th century military map, showing the location of kiln and clay pit which are marked as site “A”.

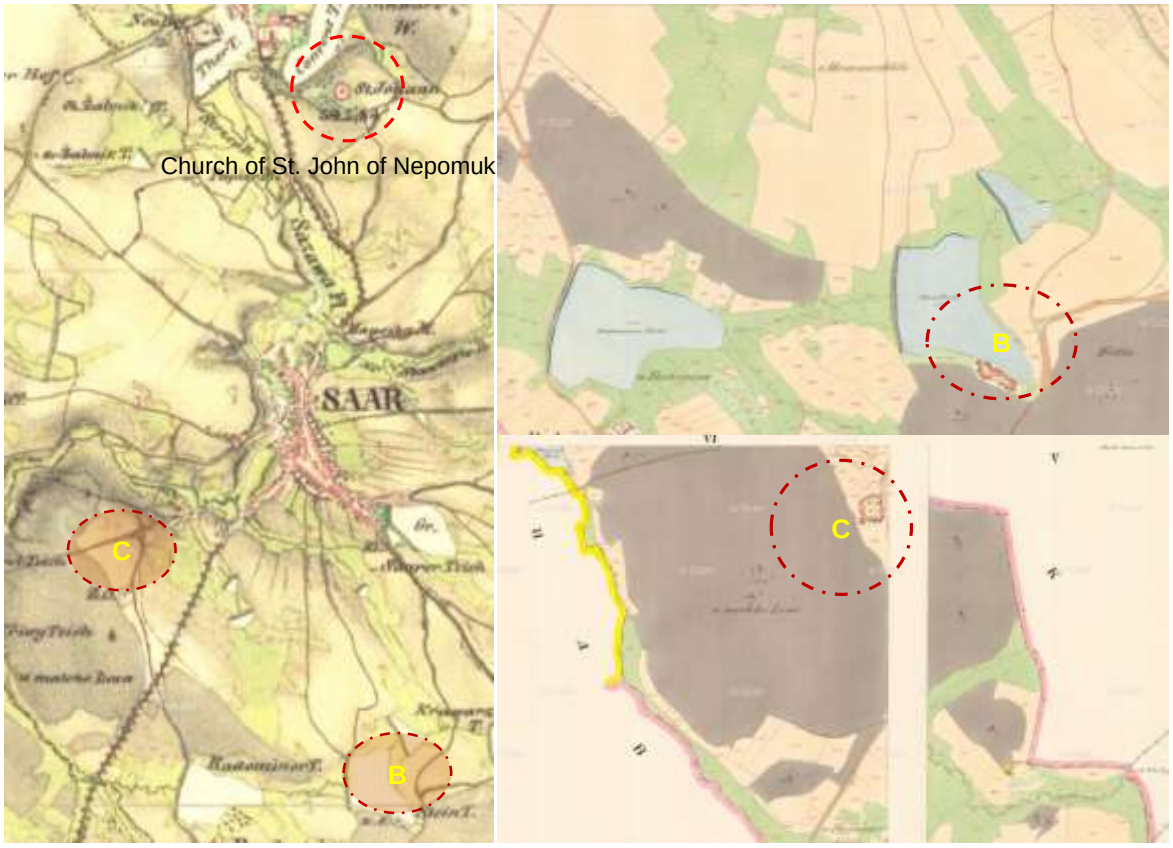

Figure 14- Cadastral maps from the first half of the 19th century highlighting the church; Oldest maps of the 2nd Military Survey come from the second half of the 18th century showing location of site “B” and “C”. (Stabilní katastr Čech - Světnov, původně Swietnow, n.d.) (Geoinformation, n.d.)

The operation of the clay pits stopped some time ago and previously quarried clay was not accessible any more. Using the notation used during that era to depict clay pits and brick kiln, using these legends, it was possible to identify the potential sites in military maps. All the three sites are located within 5 km range of the case study as shown in Figure 15.

The present location of the sites “A”, “B” and “C” in Žďár nad Sázavou is shown in Figure 15. Total of four different raw clay samples were collected. Two samples were collected from site “A” since both clay showed different texture and colours.

All four samples were collected at the depth of 30-50 cm using manual tools like shawl, not an ideal procedure. About 5 kg clay was collected for each sample. Since the area is covered in forest and grassland, the samples were contaminated with organic matter like plant roots and also had a distinct odour.

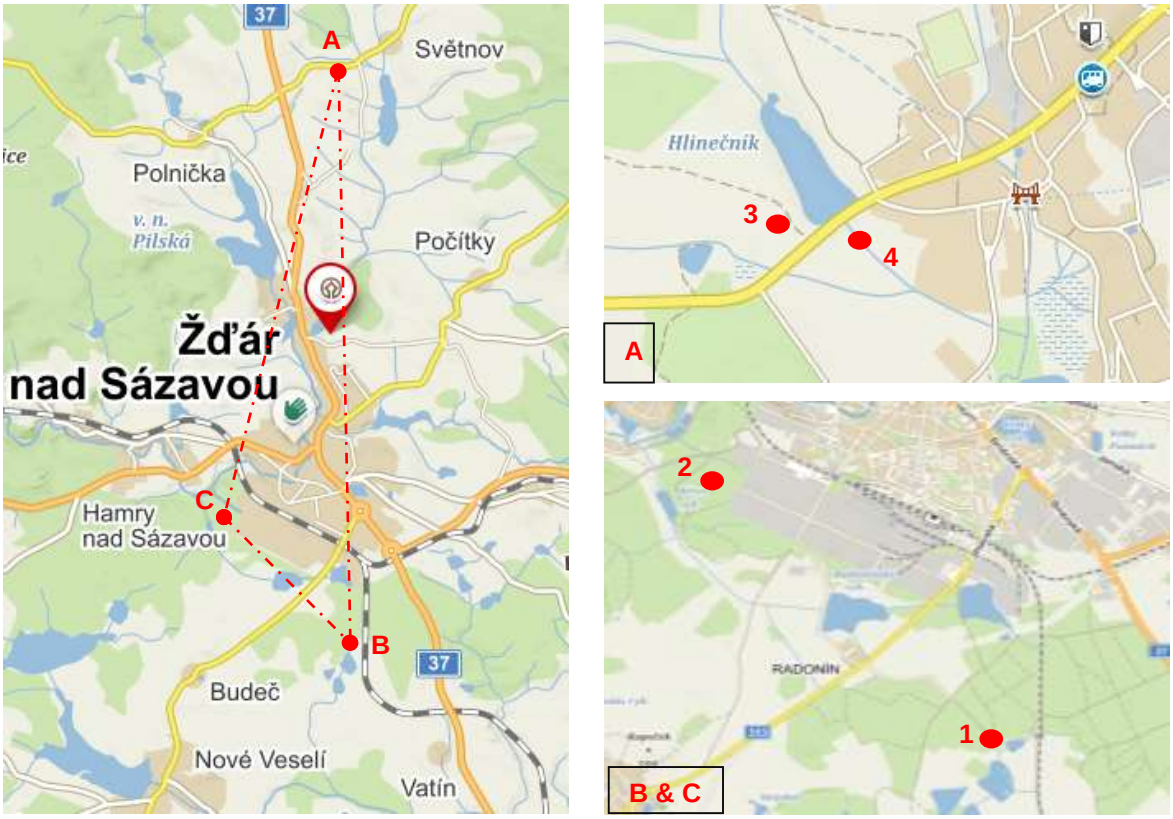

Figure 15- Present Google maps showing the location of the church and three sites "A", "B" and "C" ; Position of samples "1", "2", "3' and "4".

Presently at the location “C” there exists an industrial building as shown in Figure 15. Thus the sample was collected closest to the boundaries, keeping in account no contamination from the new construction.

4.2 Grinding and Mixing

The four different raw clay samples collected are shown in Figure 16 before drying and crushing them. The samples were cleaned from any visible organic matters (typically plant roots).

Figure 16- Raw clay samples 1, 2, 3 and 4.

Further the samples were oven dried at 105±5 °C temperature for 24 hrs. These four raw clay lumps were crushed and sieved to pass 0.8 mm sieve. Water was added to the crushed samples. Initially 15% of water compared to the total weight of respective sample was added. The workability was not achieved, hence 5% more water was added. Later for every sample the addition was between 2-3% in the third increment to achieve the required consistency. Overall the Table 2 shows the water content added for the four samples.

Table 2- Portion of water added to the four raw clay samples.

Raw Clay Sample	Water Content (% by weight)			
	1st Step	2nd Step	3rd Step	Cumulative
1	15%	5%	1.5%	21.5%
2	15%	5%	2%	22%
3	15%	5%	1%	21%
4	15%	5%	1.5%	21.5%

(a) (b) (c)

Figure 17- Mixing process; (a) Dry samples; (b) 15% by weight water addition to the samples; (c) 5% by weight water addition to the samples.

(a) (b)

Figure 18- (a) Final addition of water to the samples; (b) Covering the mixture with plastic in order to prevent evaporation.

The mixture was covered and stored so that water did not evaporate. This clay dough was tested for several filed tests to check the workability and other indicative parameters as per (Ronald Stulz, 1993).

4.3 Indicator Tests on Raw clay samples

The four raw clay samples collected were tested by simple field tests in order to verify the silt content and get assurance of the quality of the collected clay. The following tests as listed below were carried out on raw clay samples. (Ronald Stulz, 1993)

4.3.1 Water retention test

Procedure: The sample is formed into egg-sized ball after addition of required quantity of water which holds the sample together. The ball is pressed into palm and vigorously tapped by the other hand so as to shake the ball horizontally.

Indications:

- If water appears on surface after 5-10 taps and the sample ball starts crumbling, it indicates very fine sand or coarse silt.
- If the same result is obtained in 20-30 taps without crumbling of ball and flattening, this is indicative of slightly plastic silt.
- If no change or slow change observed, this indicates high clay content.

Results:

Table 3- Result of Water retention test.

Sample	No. of Taps	Result
1	10-15	Sample contains coarse silt
2	20-30	Slightly plastic sample
3	25-35	Plastic sample
4	20-30	Slightly plastic sample

4.3.2 Thread test

Procedure: Prepare moist ball and roll over flat surface to form thread, till 3 mm diameter of thread is obtained. Remould the thread into a ball and squeeze between thumb and forefinger.

Indications:

- The sample has high clay content if the ball is hard to crush.
- If the thread breaks before 3 mm, this is indicative of high silt or sand content.
- A soft spongy feel means organic soil.

Results:

Table 4- Result of Thread test.

Sample	Indication	Result
1	3 mm thread formed	Good clay content
2	Ball broke before 3 mm	High silt or sand content

Sample	Indication	Result
3	3 mm thread formed	Good clay content
4	Ball broke before 3 mm	High silt or sand content

4.3.3 Ribbon test

Procedure: Prepare cigar shape of 12 to 15 mm thickness from the sample. This shape is further progressively flattened between thumb and fore figure to form a ribbon of 3 to 6 mm thickness. Allow to grown this form.

Indications:

- No ribbon formation indicates negligible clay content.
- Ribbon of 5 to 10 cm length shows low clay content.
- Ribbon formed of 25 to 30 cm is indication of high clay content.

Results:

Table 5- Result of Ribbon test.

Sample	Indication	Result
1	10 cm	Moderate clay content
2	7 cm	Low clay content
3	17 cm	Moderate clay content
4	12 cm	Moderate clay content

Note: The results may differ depending on the quantity of water added to the clay samples.

(a) (b) (c)

Figure 19- Tests documentation for raw clay sample 1; (a) Water retention test; (b) Thread test; (c) Ribbon test result.

It can be concluded from these tests that raw clay sample 3 was more plastic while clay sample 2 had lower amount of clay and contains coarse silt. The clay samples 1 and 4 seemed compared. The tests do not assess the quality in terms of brick or tile production.

4.4 Moulding

The moulds of 40×40×160 cm were used to cast the brick specimens. EN 1015 – Mortar tests. The moulds were cleaned, greased using oil or gel and bottom was covered by thin foil so as to prevent the raw clay on sticking to the mould surface. A small amount of clay dust was sprinkled to prevent the adhesion.

(b)

Figure 20- Greased moulds of 40×40×160 cm for preparing specimens

A total of 24 specimens were moulded since for each clay sample we required five different burning temperature and one raw clay specimen. These were kept at room temperature to set for 24 hrs. The samples showed considerable shrinkable after drying and few shrinkage cracks on the surface were visible. The Table 6 shows the details of these 24 samples.

Table 6- Number of specimen w.r.t burning temperature.

Firing Temperature	Clay sample 1	Clay sample 2	Clay sample 3	Clay sample 4
650°C	1-1	2-1	3-1	4-1
750°C	1-2	2-2	3-2	4-2
850°C	1-3	2-3	3-3	4-3
950°C	1-4	2-4	3-4	4-4
1050°C	1-5	2-5	3-5	4-5
Raw Clay	1-6	2-6	3-6	4-6

After removing samples from mould, they were weighed, oven dried and measured for their dimensions. The dimension of each sample before burning can be seen in Table 7.

Table 7- Dimensions of specimens before burning process.

Specimens	Length (cm)	Breadth (cm)	Height (cm)
1-1	152.75	38.62	39.02
1-2	152.57	38.51	38.74
1-3	152.73	38.66	38.86
1-4	153.04	38.65	38.90
1-5	153.64	38.44	38.79
1-6	153.67	38.48	38.58
2-1	155.53	39.04	39.48
2-2	156.01	39.04	39.33
2-3	155.90	38.79	39.01
2-4	155.57	38.94	39.56
2-5	155.85	39.01	39.65
2-6	155.84	38.82	39.40
3-1	155.23	39.16	38.68
3-2	154.95	39.10	38.86
3-3	155.58	38.96	38.68
3-4	155.86	39.02	38.95
3-5	155.97	38.99	38.94
3-6	155.70	38.94	38.85
4-1	155.28	38.94	39.47
4-2	155.68	38.79	39.10
4-3	154.96	39.09	38.96
4-4	155.60	39.02	39.05
4-5	155.30	39.05	38.74
4-6	155.30	38.93	38.58

4.5 Burning of Specimens

The specimens were burnt/fired under controlled temperature conditions in type laboratory kiln. They were fired in set of four as the temperatures specified in Table 8. The time duration for each temperature was calculated using temperature vs. time graph. The duration of firing for each set is calculated and depicted in Table 8. The heating rate to reach the burning temperature was set to 300 °C/h. After the burning temperature was reached it was kept constant for next 3 h. The cooling phase took about 15-25 hours of time.

Table 8- Details of firing temperature, firing duration and dwelling time.

Specimens	Firing Temperature	Firing Duration	Time to reach firing temperature	Dwelling time
1-1, 2-1, 3-1, 4-1	650° C	5.2	130	180
1-2, 2-2, 3-2, 4-2	750° C	5.5	150	180
1-3, 2-3, 3-3, 4-3	850° C	5.8	170	180
1-4, 2-4, 3-4, 4-4	950° C	6.2	190	180
1-5, 2-5, 3-5, 4-5	1050° C	6.5	210	180

An additional thermocouple with a data logger was used to measure the temperature of the furnace every 1 min. Its position was just above the specimens in order to check the temperature in the furnace nearer to them, see Figure 21.

(a)

(b)

The thermocouple temperature recording is illustrated in Figure xx for 650 °C and 1050 °C temperature.

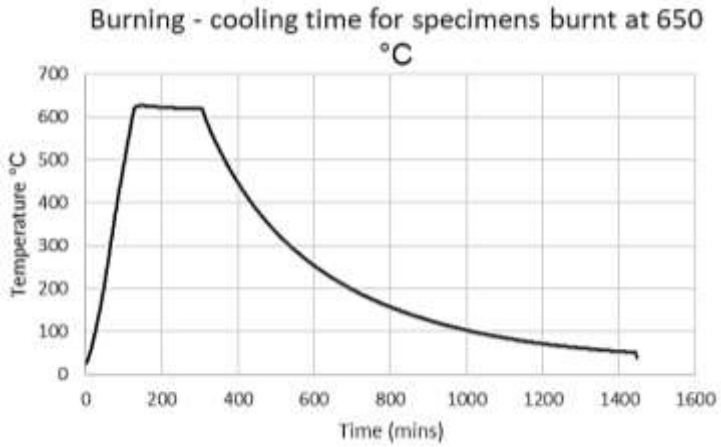

(c))

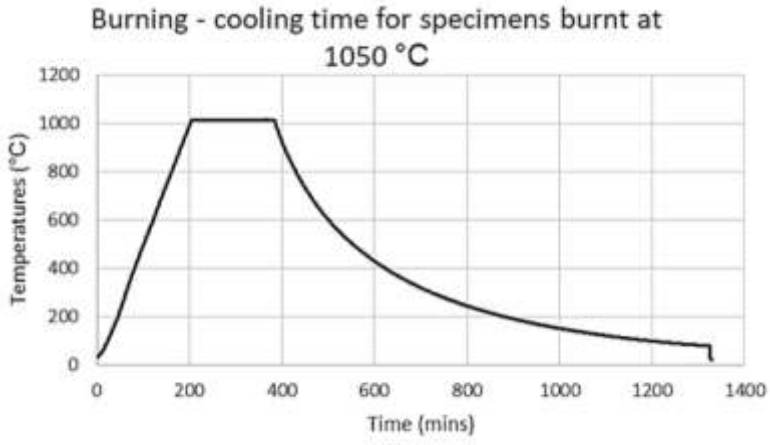

(d)

Figure 21- Thermocouple position and data for minimum and maximum burning temperature; (a) 650 °C; (b) 1050 °C.

The fired specimens of all five temperatures along with the raw clay specimens can be viewed in Figure 22. They are arranged in order of low to high burnt ceramic from left to right side respectively.

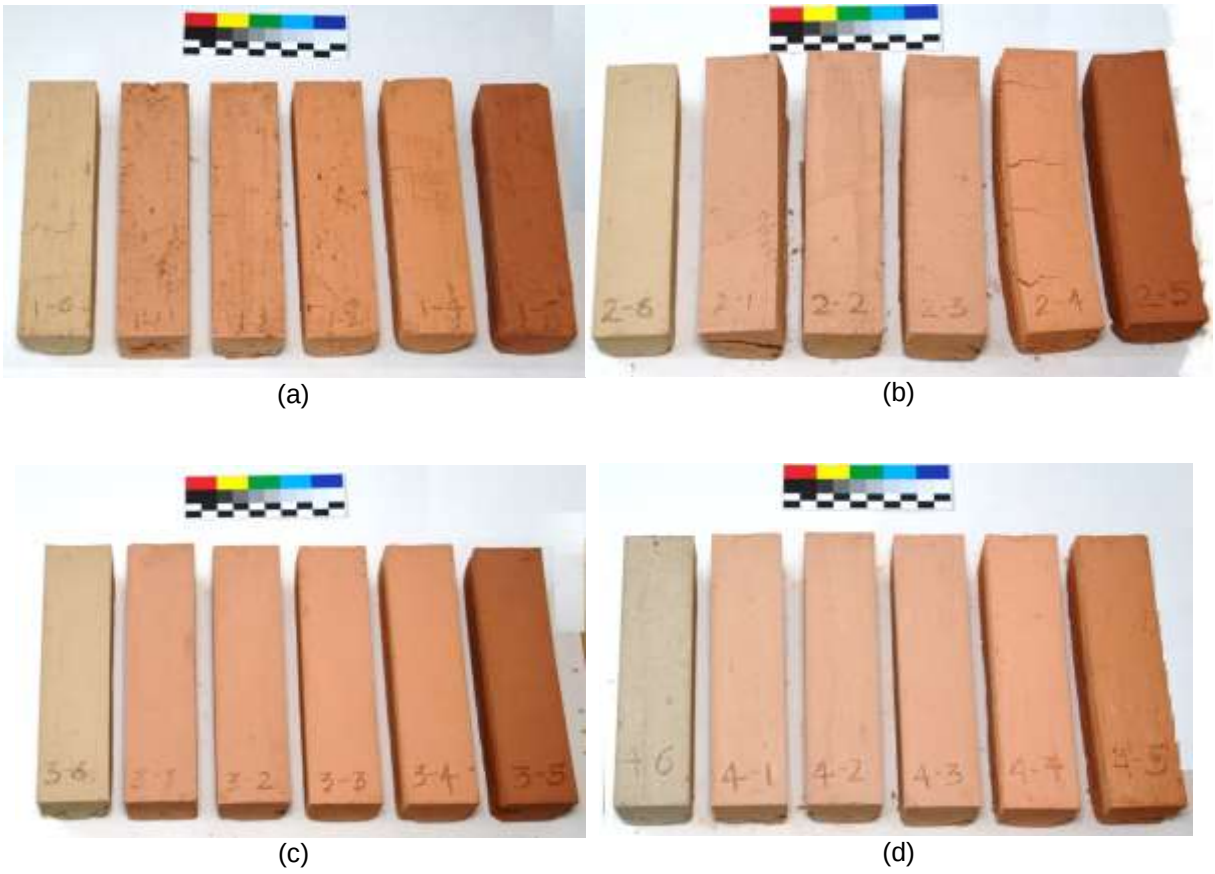

(a) (b)

(c) (d)

Figure 22- Display of burnt ceramic specimens for each clay sample burnt at different temperatures; (a) Specimens of clay sample 1; (b) Specimens of clay sample 2; (c) Specimens of clay sample 3; (d) Specimens of clay sample 4.

The specimens 2-1, 2-2, 2-3 and 2-4 prepared from sample 2 clay were cracked tremendously during firing process. The resulted specimen failure can be seen in Figure 23.

(a) (b)

Figure 23- Spalled and cracked specimens of clay sample 2; (a) Side profile; (b) Back profile.

The fired brick specimens were weighed and measured. The dimensions of the burnt specimens can be seen in Table 9.

Table 9- Dimensions of burnt specimens.

Specimens	Length (cm)	Breadth (cm)	Height (cm)
1-1	152.75	38.62	39.02
1-2	152.57	38.51	38.74
1-3	152.73	38.66	38.86
1-4	153.04	38.65	38.90
1-5	153.64	38.44	38.79
1-6	153.67	38.48	38.58
2-1	155.53	39.04	39.48
2-2	156.01	39.04	39.33
2-3	155.90	38.79	39.01
2-4	155.57	38.94	39.56
2-5	155.85	39.01	39.65
2-6	155.84	38.82	39.40
3-1	155.23	39.16	38.68
3-2	154.95	39.10	38.86
3-3	155.58	38.96	38.68
3-4	155.86	39.02	38.95
3-5	155.97	38.99	38.94
3-6	155.70	38.94	38.85
4-1	155.28	38.94	39.47
4-2	155.68	38.79	39.10
4-3	154.96	39.09	38.96
4-4	155.60	39.02	39.05
4-5	155.30	39.05	38.74
4-6	155.30	38.93	38.58

Three point bending test was performed on the specimens resulting in approximate two half pieces (x). One half used for compression test and other were cut using mechanical saw cutter, further divided in three parts which were utilized for physical-chemical tests and observations.

(a) (b)

Figure 24- Cutting the specimens for laboratory tests; (a) Mechanical saw cutter; (b) Pieces of specimens.

5. TESTS AND METHODS

This section discusses in detail the tests carried out on the specimens to obtain the mechanical and physical-chemical properties. The sample preparation and apparatus specifications and procedure for each analytical test is detailed out under this section.

5.1 Open Porosity, Water absorption, Specific density and Interconnectivity of pores

The specimens excluding the number 2 and the raw clays were tested to obtain water absorption, total open porosity and closed porosity. The specimens were oven dried at 105±5 °C for 24 hours and the dry weight was recorded as M_{dry} in grams. These dried specimens were saturated in distilled water for 24 hours and the wet weight was noted as M_{wet} in grams.

(a) (b)

Figure 25- Water absorption test; (a) dry specimens; (b) specimens saturated in distilled water.

The second step involved test for determining open porosity. The dried specimens were placed in vacuum chamber as shown in Figure 26 for 24 hours.

(a) (b)

Figure 26- Porosity test; (a) Specimens placed under vacuum; (b) specimens placed under vacuum in saturated condition.

The chamber was later filled with distilled water till the samples were submerged completely and left to saturate for 24 hours. Next step was to allow atmospheric pressure inside the vacuum chamber and leave the samples in this state for another 24 hours. The samples were weighed under water and this weight was noted as Mass $M_{sat, W}$ in grams. The same specimens were surface dried that is the surface was cleared from visible water by patting the surface using paper towel. This weight was noted as Mass $M_{sat, A}$ in grams.

For measuring specific density of ceramic specimen the SG bottles which is one of the common type of Pycnometer were used. Three different sizes of 25 ml, 50 ml and 100 ml were selected to test the specimens. The mass of cleaned and oven dried empty bottles was noted as M_1 in grams. The mass of Pycnometer and dry specimen was recorded as M_2 in grams. These Pycnometers containing specimens were half filled with distilled water and let to sit for about half hour (Figure 27).

(a) (b)

Figure 27- Pycnometer test; (a) Pycnometers with dry specimen; (b) Pycnometers half filled with water and specimen.

The entrapped air was removed and Pycnometers were carefully filled with water including the cork. The mass of Pycnometer along with specimen and water was noted as M_3 in grams. M_4 was denoted as the mass of Pycnometer containing water. The mass were measured with an accuracy of 0.001 grams. Entire procedure was carried out at temperature of 24 °C.

Figure 28- Completely filled Pycnometers.

Using equation 1 as below, the specific density of the specimens was calculated. For relative density of water at 24 °C the ASTM D8-54 provided table was used.

Table 10- Relative density of water at different temperatures (ASTM D8-54)

Temperature Degrees C	Relative Density of Water	Correction Factor K
18	0.9986	1.0004
19	0.9984	1.0002
20	0.9982	1.0000
21	0.9980	0.9998
22	0.9978	0.9996
23	0.9975	0.9993
24	0.9973	0.9991
25	0.9970	0.9989
26	0.9968	0.9986
27	0.9965	0.9983
28	0.9963	0.9980
29	0.9960	0.9977
30	0.9957	0.9974

$$\rho = \frac{(m_2 - m_1) \cdot \rho_s}{m_4 - m_3 - m_1 + m_2} \quad (1)$$

Where:

M_1 = weight of dry pycnometer, g

M_2 = weight of pycnometer with dry sample of sand, g

M_3 = weight of pycnometer filled with water and soil at room temperature T, g

M_4 = weight of pycnometer filled with water, g

ρ = relative water density at °C

The degree of interconnectivity of pores which is function of total porosity stating the percentage of pore connectivity, can also be useful indication for closed pore. Using free water absorption and forced water absorption, the degree of pore interconnectivity can be calculated as shown in equations 2, 3 and 4.

$$Free\ water\ absorption\ Fr\ (\%) = \frac{(M_{wet} - M_{dry})}{M_{dry}} \times 100 \quad (2)$$

$$Forced\ water\ absorption\ Fo\ (\%) = \frac{(M_{sat,A} - M_{dry})}{M_{dry}} \times 100 \quad (3)$$

$$Degree\ of\ pore\ interconnectivity = \frac{(Fo - Fr)}{Fo} \times 100 \quad (4)$$

5.2 Flexural and Compressive strength tests

Three point bending test was carried on all the specimens except for specimens of clay sample 2 as they were spalled and cracked. The test used load cell of 25 kN capacity. The speed of loading was 0.15 mm/min.

Figure 29- Three point bending test in progress for specimen 1-3.

The compressive strength test was carried out using potentiometer under load cell of 25 kN capacity for specimens burnt up to 950 °C at loading speed of 0.45 mm/min. The load cell was changed to 100 kN for specimens burnt at 1050 °C as they exceeded 25 kN threshold, thus it should be noted that specimens 1-5, 3-5 and 4-5 underwent two cycles of loading.

The common cracking pattern observed was apple-core cracking in all specimens.

(a) (b)

Figure 30- Compressive strength test on specimen 1-1 and failure pattern.

5.2 X-ray Diffraction and QPA

To obtain the chemical-mineralogical content of the specimens, X-ray diffraction was performed on the specimens. The samples including original tile from the church, raw clay and fired specimens were dried at 105±5 °C overnight, grounded and homogenized by hand. Small amount from sample was then grounded in ball mill by setting the apparatus at 30 vibrations for 4 minutes as shown in Figure 31 and for burnt samples 30 oscillations for 6 minutes to obtain fine homogeneous powder.

(a) (b)

Figure 31- Grounding sample for XRD; (a) ball mill and raw clay sample 1; (b) fine grinding using mechanical ball mill.

The burnt clay brick powder samples were spiked by addition of weighed standard- corundum (aluminium powder) (Barua, 2013). This benefits in knowing the amorphous content. A mixture of 0.45 gram of sample powder and 0.05 gram of corundum was prepared by weighing with an accuracy of 0.0001 g Figure 32.

(a) (b) (c)

Figure 32- Mixing standard with brick powder; (a) 0.45 g brick sample; (b) 0.05 g corundum powder; (c) Mixing homogeneously.

The resulting intensities after addition of corundum were filtered using software TOPAS 4.2 (Bruker AXS). The samples were loaded in the sample holders in a randomly orientated way to minimize preferred orientations of clay minerals. Preferred orientation is an extreme case of non-random distribution of the crystallites which distorts the intensities that are used for analysis. Glass slide was pressed on the sample holder and the sample holder was tapped in order to overcome preferred orientation. The samples were loaded from side. The software also rectifies the error of preferred orientations (ThermoARL, 1999). A refinement has be applied to the graph obtained in order to avoid difficulties. Preferred orientation can be checked and the parameters can be set for crystals orientation and directions in the software. The sample holder and all apparatus were cleaned by water and acetone to avoid contamination of samples. The sample holder and machine are shown in Figure 33.

(a) (b) (c)

Figure 33- Sample holder and loading; (a) Using glass slide to load sample; (b) fully loaded sample holder for raw clay 2-6; (c) X-ray diffraction machine set up.

Data were collected in the angular range 4-82° 2θ using a Bragg-Brentano θ-θ diffractometer, Cu Kα radiation (λ= 1.5418 Å), equipped with a LynxEye 1-D silicon strip detector, at 40 kV and 40 Ma. Divergence 0.6 mm slit and 2.5° Soller slits were mounted on the incident beam pathway. The pathway of the diffraction beam included a Ni filter and Soler slits (2.5°). A virtual step scan of 0.0102° 2θ with 0.4s/step counting time was implemented (Alberto Viani, 2016). The intensities were measured for about two hours for each sample. The machine was ran in steps. The machine can be loaded with fifteen sample holder at a time. The results were derived and the software TOPAS 4.2 (Bruker AXS) was informed about the amount of standard present and the data from the stored data log was used to identify the prominent peaks appearing in this graph.

5.3 Thermal analysis

Thermogravimetric analysis (TG) and derivative thermal analysis (DTG) were applied for the characterization of the four raw clay samples and the outcomes obtained are detailed out in this section. Thermal analysis was carried out on all the four raw clay samples. The sample for analysis was prepared by measuring 10 gram representative part of the raw clay sample on a weighing scale with accuracy 0.0001 grams. This prepared sample was carefully placed in the thermal analysis furnace (Figure 34). Thermal analysis was performed with a BÄHR Thermo analyse STA 504 instrument, using alumina crucible, N2 gas flow, heating rate of 20 °C/min and temperature range 20 – 1100 °C. The machine was attached to computer that recorded the Thermogravimetric analysis (TG) and Derivative thermal analysis (DTA) data.

Figure 34-BÄHR Thermo analyse STA 504 instrument.

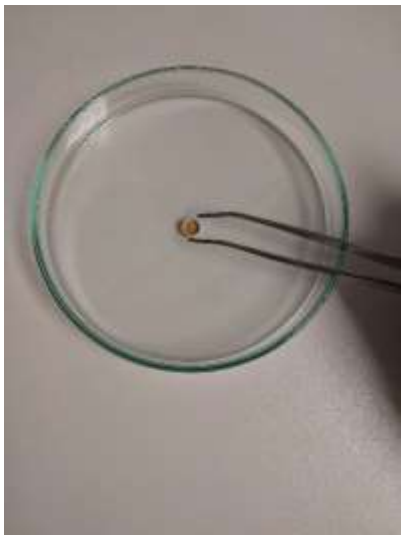

(a)

(b)

Figure 35- Sample preparation for thermal analysis; (a) 10 gram of raw clay prepared for testing; (b) carefully placing the sample in the furnace.

5.4 Optical Microscopy

The petrographic analysis was carried out using Olympus BX41. Thin sections were prepared using a small piece of 0.5 g weight and dimension of 3.5 cm to 4 cm. Initially a small chip was prepared from the cut section of the specimen. After drying the chip was placed with cut face upwards and drizzled with epoxy (impregnation of sample). The surface was polished using silicon carbide powder and was washed thoroughly under water jet. This polished chip was bonded to glass slide and the majority of chip was cut for re-sectioning in thin section machine. The thin section machine cut the chip using a diamond tipped cutting wheel (Quinn, 2013). The thin section was washed and viewed under the microscope. Thin sections for all specimens were prepared using this procedure. The thin section was viewed under polarized light for better understanding of different minerals (Figure 36 & 37).

(a) (b)

Figure 36- (a) prepared thin section; (b) portrait position of section under microscope.

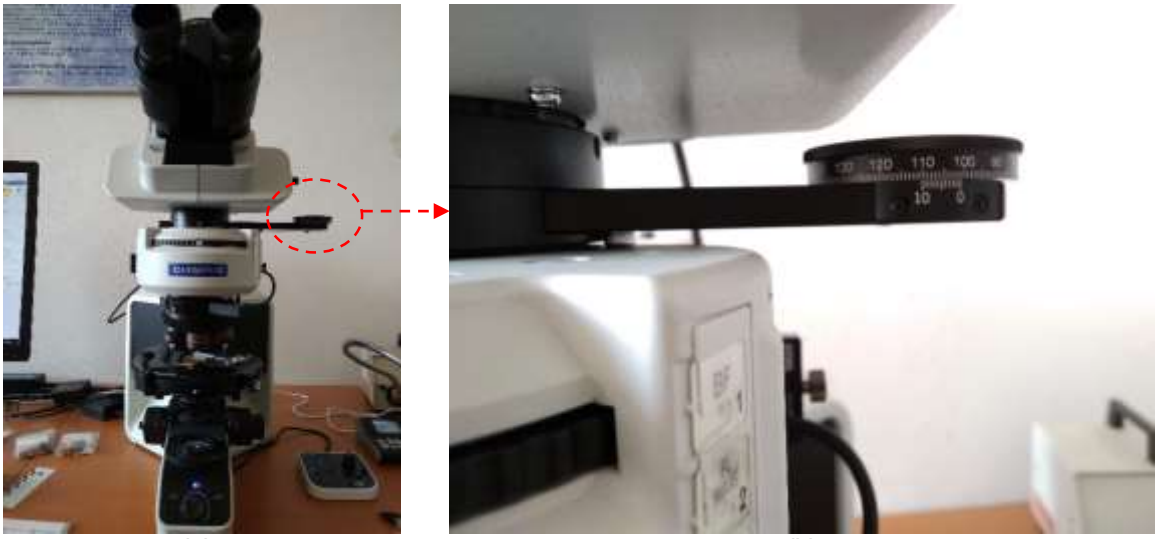

(a) (b)

Figure 37- (a) Olympus BX41; (b) polarized light filter.

6. RESULTS

6.1 Open Porosity, Water absorption, Specific gravity and Pore interconnectivity

The open porosity % vol. was calculated for all the specimens excluding the raw clay specimen and specimens prepared from sample 2. The results for original tiles were obtained along with the others.

Table 11- The volume of open pores, volume of specimens and % of open porosity.

Specimen	Volume of open pores (cm^3)	Volume of sample (cm^3)	Open porosity % vol.
1-1	16.1	43.96	36.6
1-2	17.0	46.47	36.6
1-3	17.1	46.55	36.7
1-4	16.4	44.87	36.5
1-5	12.9	41.58	31.0
3-1	14.9	43.45	34.4
3-2	14.7	42.17	34.8
3-3	15.6	44.55	35.0
3-4	15.1	43.74	34.6
3-5	12.7	43.40	29.4
4-1	15.8	45.49	34.7
4-2	15.1	43.70	34.6
4-3	15.5	44.37	34.8
4-4	16.8	47.33	35.5
4-5	14.7	44.44	33.1
Original tile	12.7	44.26	28.7

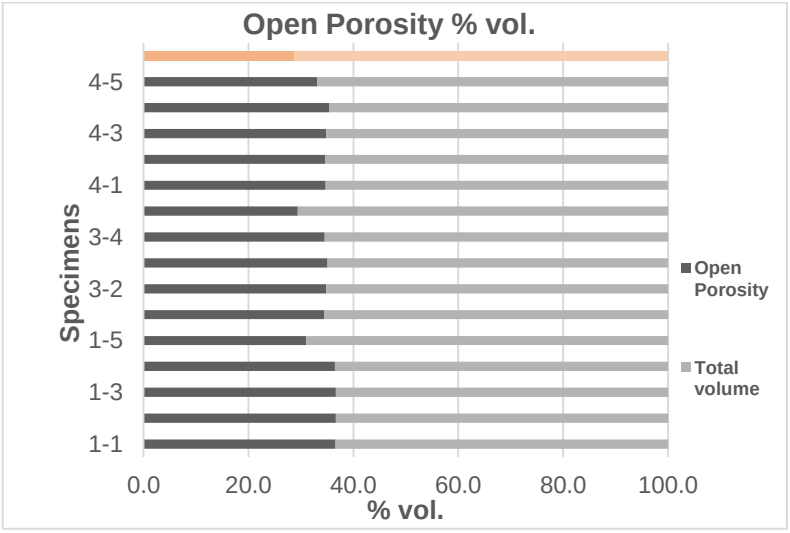

Figure 38- The open porosity % vol. of all specimens and the original tile.

The open porosity %vol. was less for specimens burnt at 1050 °C compared to other specimens for all samples. The porosity for specimens burnt at 850 °C that is 1-3, 3-3 and 4-3 was observed to be highest than the rest of the specimens.

Using the data of dry weight of specimen, saturated weight and immersed weight to calculate free-forced absorption, the degree of pore interconnectivity was calculated as described in the Tests and methods chapter.

Table 12- Degree of pore interconnectivity for a specimens of clay sample 1, 3, and 4, and original tile.

Specimens	Free absorption Wt.%	Forced absorption Wt.%	Degree of pore interconnectivity Wt.%
1-1	17.6	21.3	17.14
1-2	17.8	21.3	16.52
1-3	17.8	21.3	16.77
1-4	17.5	21.2	17.42
1-5	12.9	16.8	23.18
3-1	16.2	19.5	17.00
3-2	16.5	19.9	17.22
3-3	16.5	20.1	17.87
3-4	16.2	19.7	17.41
3-5	11.6	15.7	25.71
4-1	16.2	20.0	19.09
4-2	16.2	19.9	18.60
4-3	16.3	20.2	19.69
4-4	16.5	20.8	20.46
4-5	14.1	18.7	24.51
Original tile	12.6	15.2	17.32

The degree of pore interconnectivity is a function of total porosity, hence cannot be directly related to the open porosity. The results here state that specimens burnt at high temperature; 1-5, 3-5 and 4-5 possess higher degree of porosity (23-26%) than the other specimens. The higher the difference between forced absorption and free absorption, higher is the degree of pore interconnectivity which indicates more number of difficult to access pores (Giuseppe Cultrone *. I., 2005). The degree of pore interconnectivity can be related to permeability as suggested by Giuseppe, 2005.

The specific density calculated from pycnometer test gave result in the range of 2.4-2.7 kg/m^3 for all the specimens except for specimens of sample 2. The free water absorption for specimen s 1-5, 3-5 and 4-5 was noted as 12.9, 11.6 and 14.1 % while the original brick showed 12.6 %.

It should be noted that the pycnometer test was not carried on the original tile since it was limited.

6.2 Mechanical Properties

The flexural and compressive strength tests were carried out on the burnt clay and raw clay specimens to understand the overall bearing capacity. These tests were not performed for specimens of clay sample 2 as the specimens were cracked and not in in ideal state. The original tile specimen was limited and valuable for tests like XRD and optical microscopy and porosity.

6.2.1 Flexural tests results

For flexural strength test, typical load verses time graph for selected burnt ceramic specimens (minimum and maximum flexural strength) are displayed below. The peaks depict brittle failure.

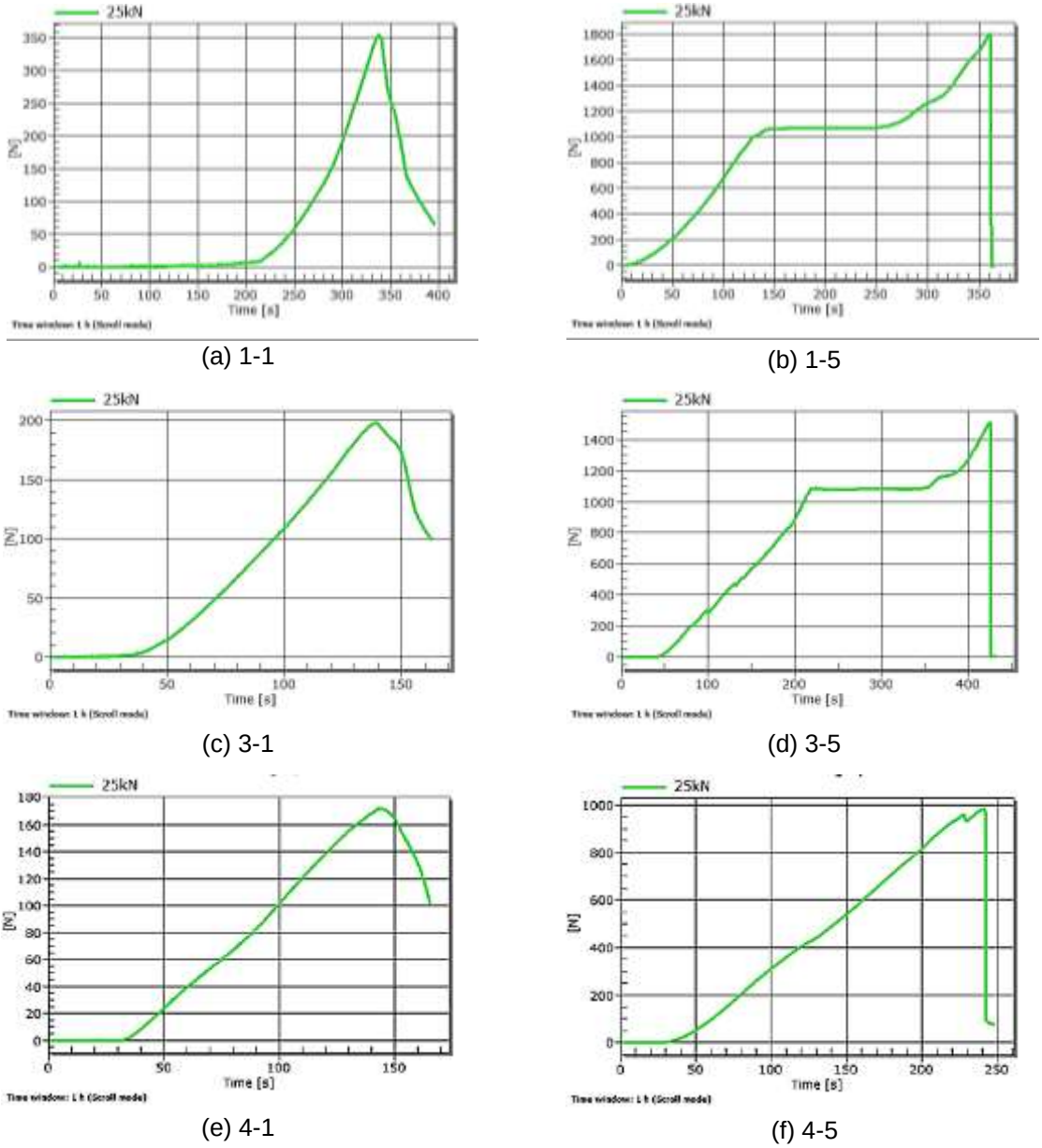

(a) 1-1 (b) 1-5

(c) 3-1 (d) 3-5

(e) 4-1 (f) 4-5

Figure 39- Load verses time graph for minimum and maximum temperatures of burnt ceramic specimens

A very prominent plateau mainly caused by residual resistance was observed for 1-5 and 3-5, the specimens burnt at high temperature (1050 °C). The specimens burnt at 650-750 °C, 850-950 °C and 1050 °C possessed flexural strength in similar range. The highest flexural strength for all temperatures was obtained by specimens prepared from raw clay sample 1 as shown in Figure 40.

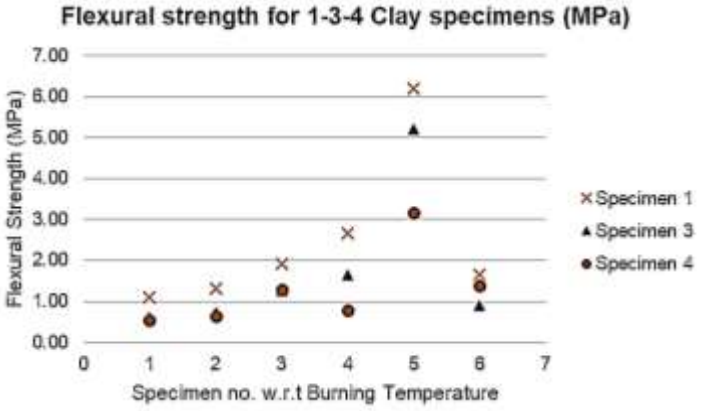

Figure 40- Flexural strength achieved by the burnt and raw clay specimens for sample 1, 3 and 4.

6.2.2 Compressive strength results

The compressive test results for burnt and raw specimens were obtained and graphically presented in Figure 41. The maximum compressive strength was obtained for the specimens burnt at 1050 °C. The specimen 1-5 attained a compressive strength of 20.65 MPa. On the other hand, the specimens of clay sample 4 achieved moderate compressive strength results.

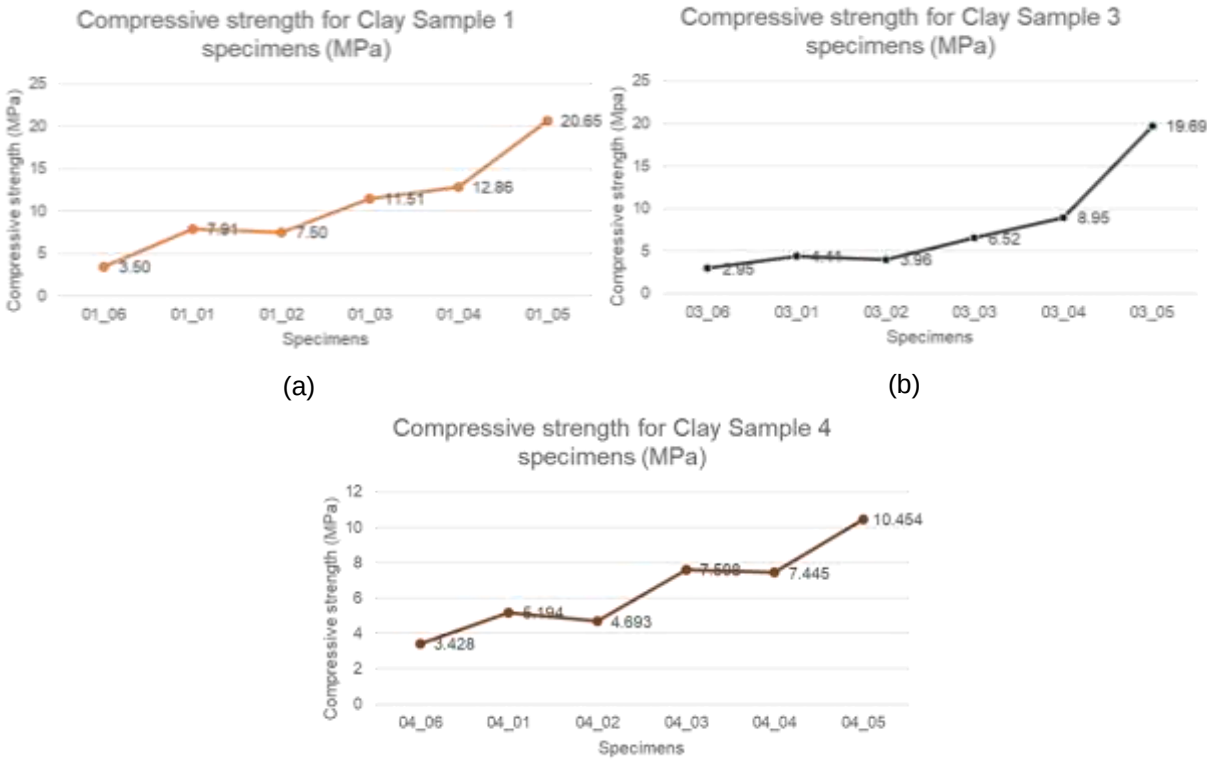

Figure 41- Compressive strength achieved by Clay sample 1, 3 and 4 specimens.

Comparison of compressive strength and porosity

The specimens with burning temperature 650-750 °C and 850-950 °C had compressive strength within similar range for specimens of clay sample 1 and 4. However the specimens of clay sample 3 possessed a wider range. The specimens with high compressive strength showed low open porosity but high degree of pore interconnectivity. The specimen 4-5 had compressive strength of 10.45 MPa with open porosity of 33% and 24.5 % degree of pore interconnectivity.

Table 13- Compressive strength, porosity and degree of pore interconnectivity for all specimens.

Specimens	Compressive strength MPa	Open porosity %	Degree of pore interconnectivity Wt.%
1-1	7.91	36.6	17.14
1-2	7.50	36.6	16.52
1-3	11.51	36.7	16.77
1-4	12.86	36.5	17.42
1-5	20.65	31.0	23.18
3-1	4.41	34.4	17.00
3-2	3.96	34.8	17.22
3-3	6.52	35.0	17.87
3-4	8.95	34.6	17.41
3-5	19.69	29.4	25.71
4-1	5.194	34.7	19.09
4-2	4.693	34.6	18.60
4-3	7.598	34.8	19.69
4-4	7.445	35.5	20.46
4-5	10.454	33.1	24.51

The relation between compressive strength, porosity and degree of pore interconnectivity can be seen in Table 13. A direct relation was observed between compressive strength and porosity. The change in compressive strength w.r.t to burning temperature can be accounted by the microstructure changes occurred within the specimen.

6.3 X-ray diffraction

XRD and QPA provide the mineralogical components of the specimens and results obtained from software TOPAS 4.2 are displayed in the tables below.

Clay sample 1

For clay sample 1, the raw specimen 1-6 was dominant with quartz and combined with feldspar they constitute about 75 wt%. The presence of albite, kaolinite, vermiculite and muscovite is significant. Chlorite, amphibole and Pargasite constitute about 3.8 wt%.

Table 14- Quantitative phase analysis (wt%) of burnt and raw clay specimens for sample 1.

Phase (%)	Raw Clay	Fired Specimens					Original Burnt clay unit
		650 °C	750 °C	850 °C	950 °C	1050 °C	
	1-6	1-1	1-2	1-3	1-4	1-5	
Quartz	64	49.4	52.8	56.2	54	50	43.4
Calcite	-	-	-	-	-	-	-
Albite	6	4.8	4	2.1	1.9	1	2.8
Ca-Feldspar	2.3	1.9	5.5	9.4	3.2	2	1.8
K-Feldspar	9.1	6	6.1	6.5	6.9	4.2	6.3
Muscovite	3.5	3	1.9	1.7	0.5	-	1.7
Hematite	-		-	-	1.8	3.2	-
Kaolinite	5.3		-	-	-	-	-
Chlorite	1.7	0.5	-	-	-	-	-
Phlogopite	-	3.7	2.8	2.8	1.6	0.5	1.6
Amphibole	1.6	1.1	1	1.5	1	-	0.6
Pargasite	0.5	0.7	1.9	1.6	1.4	-	-
Vermiculite	6	1.3	-	-	-	-	-
Amorphous	-	27.7	24	18.2	27.7	39.1	41.8
Total	100	100.1	100	100	100	100	100

The quartz remain almost constant in all five burnt specimens. They constitute about 50 wt%. Kaolinite is transformed to meta-kaolinite at about 573°C which is free amorphous. The amorphous content was obtained around 24-27 wt% for specimens burnt until 950 °C and for the highest temperature at 1050 °C it was noted as 41.8 wt%. Phlogopite was determined at 650 °C and gradually decreased with increase in firing temperature. Vermiculite disappeared at 750 °C. Amphibole and Pargasite decomposed at 1050 °C. Hematite appeared at high temperatures in specimen 1-4 and 1-5. Albite and feldspar considerably decrease at high firing temperature. The Rietveld refinement graphical output for 1-1 and 1-5 can be seen in Figure 42. The initial peaks of clay minerals disappeared at high temperature.

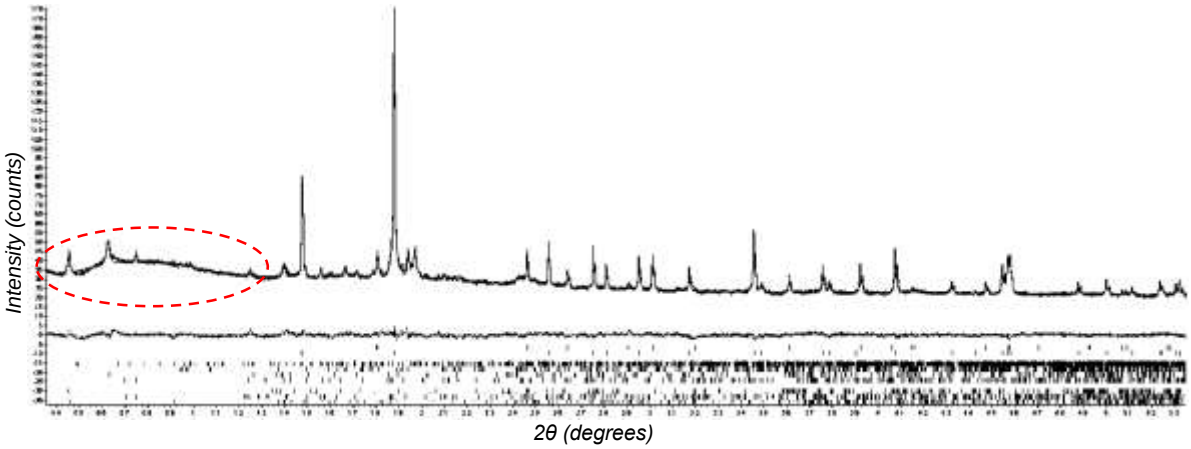

Figure 42- Rietveld refinement graphical output relative to specimen 1-1.

For both the specimens quartz is the most dominant mineral and evident in the graphs.

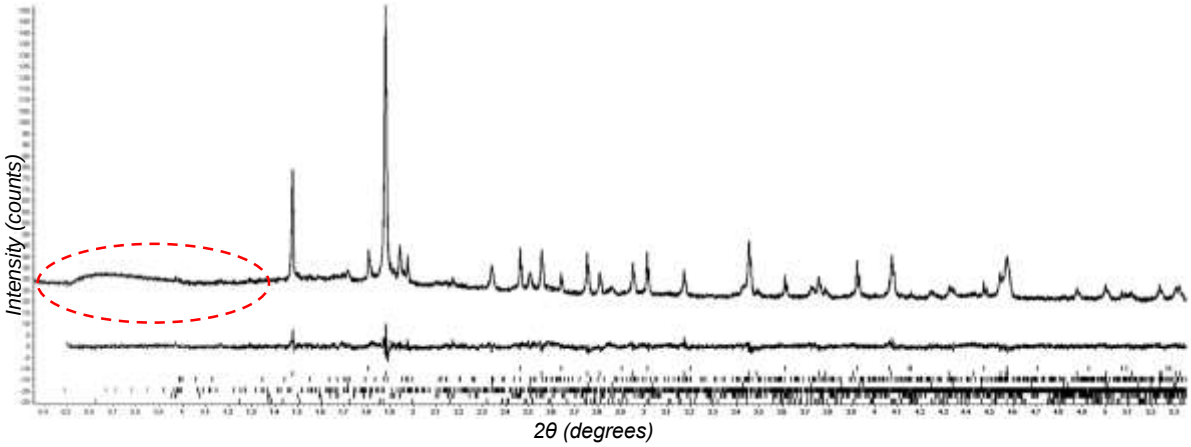

Figure 43- Rietveld refinement graphical output relative to specimen 1-5.

Clay sample 2

The raw clay specimen of sample 2 shows similar constituents as raw clay sample 1. Muscovite is not present. The amorphous proportion is low compared to 2-4 and 2-5 specimens. The content of Phlogopite for 2-1, 2-2 and 2-3 is very high, for low temperatures it is greater than quartz content.

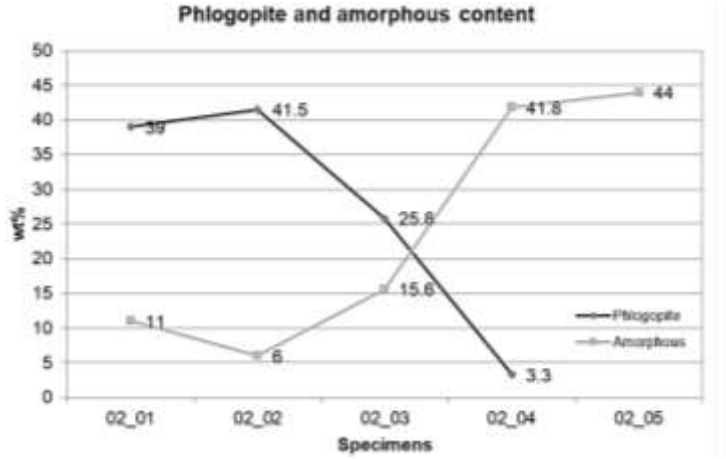

Figure 44- The amount of Phlogopite and amorphous with increase in temperature for specimens of sample 2.

Table 15- Quantitative phase analysis (wt%) of burnt and raw clay specimens for sample 2.

Phase (%)	Raw Clay	Fired Specimens					Original Burnt clay unit
		650 °C	750 °C	850 °C	950 °C	1050 °C	
	2-6	2-1	2-2	2-3	2-4	2-5	
Quartz	54.6	34.8	39.1	42.3	39.1	41.1	43.4
Calcite	-	1	-	-	-	-	-
Albite	9.5	5.2	7.5	6.7	5.8	4.5	2.8
Ca-Feldspar	9.4	2.5	1.8	3.1	3.4	4.4	1.8
K-Feldspar	7.5	3.8	3	4.6	3.8	2.3	6.3
Muscovite	6.9	-	-	-	-	-	1.7
Hematite	-	-	-	0.7	1.7	3.7	-
Kaolinite	4.1	-	-	-	-	-	-
Chlorite	0.3	0.6	-	-	-	-	-
Phlogopite	-	39	41.5	25.8	3.3	-	1.6
Amphibole	1.9	-	-	-	-	-	0.6
Pargasite	1.4	1.4	1.1	1.1	1.1	-	-
Vermiculite	4.4	0.7	-	-	-	-	-
Amorphous	-	11	6	15.6	41.8	44	41.8
Total	100	100	100	99.9	100	100	100

The albite content of this clay sample is higher compared to other samples. Hematite appeared in specimens 2-3, 2-4 and 2-5. The content of Pargasite remained constant, ultimately disappearing at 1050 °C. Chlorite is present in specimen burnt at 650 °C.

Clay sample 3

The raw clay specimen showed quartz and feldspar as its chief minerals constituting about 71 wt% followed by albite that constituted 9.5 wt%. For specimens prepared from clay sample 3, the quartz content remained in similar range till specimen 3-4 and reduced slightly for specimen 3-5.and Muscovite disappeared at high temperature and presence of hematite was observed at 950-1050 °C.

Phlogopite reduced considerably for specimen 3-4 and disappeared in specimen 3-5. Amphibole depicted a very negligible and constant content in all the specimens. The amorphous content for specimens of sample 3 clay was low in comparison to specimens of sample 1 but is similar as the content of specimens of clay sample 4. It is to be noted that for specimen 3-3, the amorphous content decreased to 12.3 wt% from 15.8 wt% of specimen 3-2 and for specimen 3-4 was noted as 18.3 wt% as shown in Figure 45.

Table 16- Quantitative phase analysis (wt%) of burnt and raw clay specimens for sample 3.

Phase (%)	Raw Clay	Fired Specimens					Original Burnt clay unit
		650 °C	750 °C	850 °C	950 °C	1050 °C	
	3-6	3-1	3-2	3-3	3-4	3-5	
Quartz	64.2	56.2	57	62.9	60.4	51.1	43.4
Calcite	-	-	-	-	-	-	-
Albite	8.4	5.2	5	3.2	1.7	0.8	2.8
Ca-Feldspar	2.1	1.6	6.5	6.7	5.1	2.6	1.8
K-Feldspar	8.1	8	8.9	8.1	10.2	4.7	6.3
Muscovite	5.7	2.4	2.5	2	0.7	-	1.7
Hematite	-	-	-	-	1.4	2.1	-
Kaolinite	4.3	-	-	-	-	-	-
Chlorite	1.1	0.3	-	-	-	-	-
Phlogopite	-	4.4	3.9	4.2	1.5	-	1.6
Amphibole	0.9	0.7	0.5	0.7	0.7	0.7	0.6
Pargasite	1	1.7	-	-	-	-	-
Vermiculite	4.3	0.9	-	-	-	-	-
Amorphous	-	18.6	15.8	12.3	18.3	38.1	41.8
Total	100.1	100	100.1	100.1	100	100.1	100

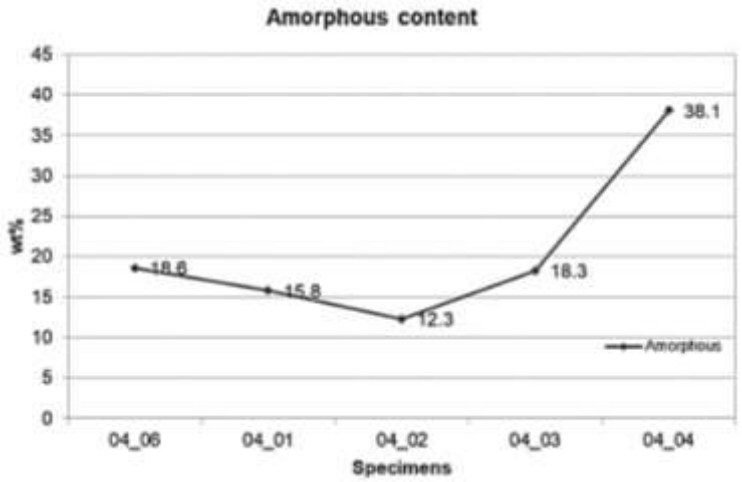

Figure 45- The amount of amorphous with increase in temperature for specimens of sample 3.

Clay sample 4

For raw clay sample 4 the quartz and feldspar together amounted to 73 wt% followed by albite at 7.5 wt%. The specimens showed slight variations in amount with increase in temperature for quartz.

Albite showed a consequent decrease. The content of K-feldspar increased with temperature as shown in Figure 46. Muscovite disappeared for specimen 4-5 and hematite appeared for 4-4 and 4-5 specimens. Chlorite was noted in specimens 4-1, 4-2 and 4-3. Pargasite remained almost constant for specimens 4-1, 4-2 and 4-3, before disappearing for specimen 4-4.

Table 17- Quantitative phase analysis (wt%) of burnt and raw clay specimens for sample 4.

Phase (%)	Raw Clay	Fired Specimens					Original Burnt clay unit
		650 °C	750 °C	850 °C	950 °C	1050 °C	
	04_06	04_01	04_02	04_03	04_04	04_05	
Quartz	62.9	56.2	56.2	52.1	56.4	55.3	43.4
Calcite	-	-	-	-	-	-	-
Albite	7.5	6.2	5.8	4.7	3.3	2.2	2.8
Ca-Feldspar	1.6	1.9	1.7	1.7	1.4	1.5	1.8
K-Feldspar	12.4	8.2	9.8	9.2	10.2	10.6	6.3
Muscovite	4.4	2.4	2.4	2.1	0.9	-	1.7
Hematite	-	-	-	-	0.5	1	-
Kaolinite	4.9	-	-	-	-	-	-
Chlorite	1.2	0.1	0.4	0.6	-	-	-
Phlogopite	-	3.8	3.1	3.7	1.4	-	1.6
Amphibole	0.9	0.6	-	-	-	-	0.6
Pargasite	1	1	1.2	1	-	-	-
Vermiculite	3.4	0.9	-	-	-	-	-
Amorphous	-	18.8	19.4	25	25.9	29.4	41.8
Total	100.2	100.1	100	100.1	100	100	100

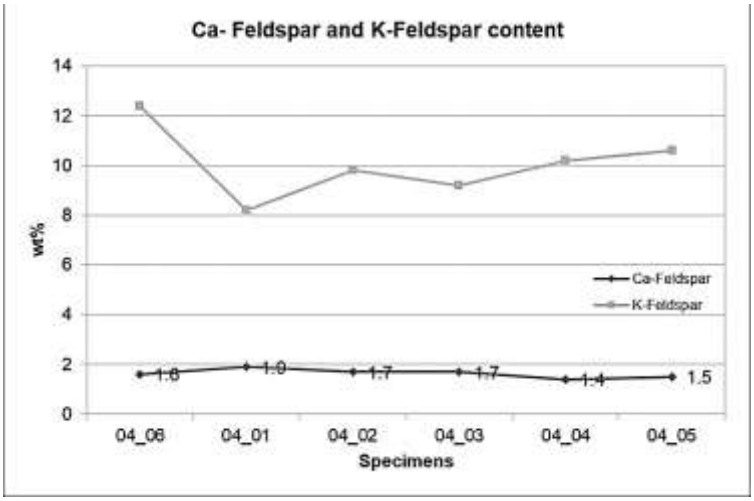

Figure 46- Ca-Feldspar and K-Feldspar content with increase in temperature for specimens of clay sample 4.

It should be noted that there was no amorphous content present in all four raw clay samples.

Comparison of mineralogy of burnt specimens

The quartz content for clay samples 1 and 3 showed a gradual increase till temperature 850 °C and reduced for higher temperatures as shown in Figure 47. But the clay samples 2 and 4 showed different trend.

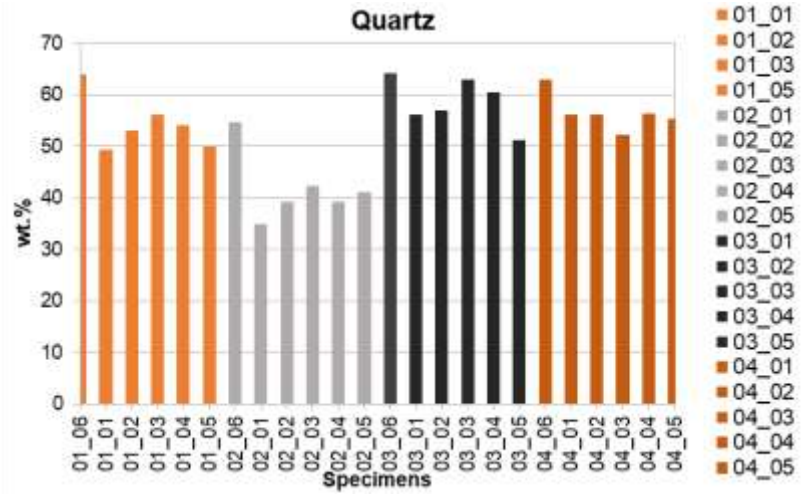

Figure 47- Quartz content for all specimens.

The Figure 48 shows the high albite content for specimens of clay sample 2 compared to the specimens of other clay samples. For all specimens the albite content drops after 750 °C.

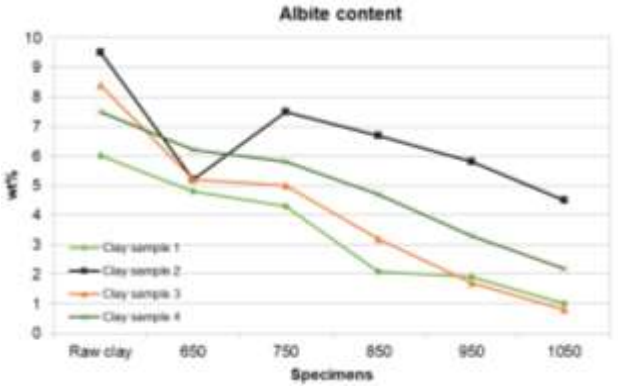

Figure 48- Albite content for all specimens.

The Phlogopite content in specimens of clay sample 2 was observed to be high and this can be the result of spalling and cracking observed in specimens.

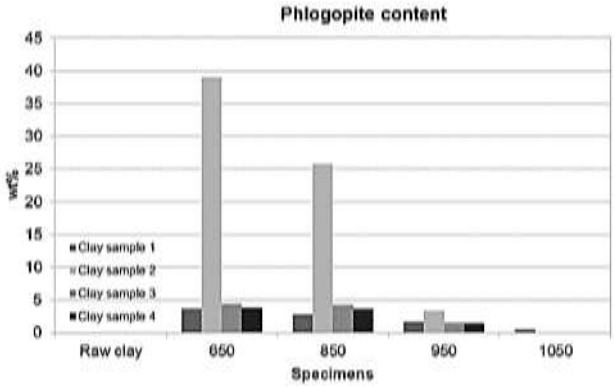

Figure 49- Phlogopite content for all specimens.

6.4 Thermal analysis

As stated by Fierascu (2009), the thermal behaviour of materials like bricks is coherent with their chemical and mineralogical composition. Thus using Universal analysis software, the Thermogravimetric (TG) curve and the Derivative thermal analysis graphs were obtained to understand the firing temperatures and transformations. For all the samples the temperature window selected was 30-1050 °C.

The mineral composition of the raw materials is known from the XRD analysis and the mineralogical composition is summarised below in Table 18

Table 18- Mineralogical composition of the raw clays.

Phase		**1**	**2**	**3**	**4**
Quartz	Silica minerals	64	54,6	64,2	62,9
	SiO_2				
Albite	Tectosilicates -feldspars	6	9,5	8,4	7,5
	$NaAlSi_2O_8$				
Ca-feldspar	Tectosilicates -feldspars	2,3	9,4	2,1	1,6
	$CaAl_2Si_2O_8$				
K-Feldspar	Tectosilicates -feldspars	9,1	7,5	8,1	12,4
	$KAlSi_3O_8$				
Muscovite	Phyllosilicates - micas	3,5	6,9	5,7	4,4
	$KAl_2[Si_3AlO_{10}(OH,F)_2]$				
Kaolinite	Phyllosilicates - clays	5,3	4,1	4,3	4,9
	$Al_2Si_2O_5(OH)_4$				
Chlorite	Phyllosilicates - clays	1,7	0,3	1,1	1,2
	$(Mg, Fe)_5Al(Si, Al)_4O_{10}(OH)_8$				
Vermiculite	Phyllosilicates - clays	6	4,4	4,3	3,4
	$(Mg,Fe{+}{+},Al)_3(Al,Si)_4O_{10}(OH)_2{\bullet}4(H_2O)$				
Amphibole	Inosilicates	1,6	1,9	0,9	0,9
	$(Ca,Na,K)_0{-}3[(Mg,Fe,Mn,Al,Ti)_5{-}7(Si,Al)_8O_{22}(O,OH,F)_2]$				
Pargasite	Inosilicates	0,5	1,4	1	1
	$NaCa_2(Mg_4Al)(Si_6Al_2)O_{22}(OH)_2$.				

The main phases containing chemically bound water are in the group of phyllosilicates (clays and micas). Their main thermic reactions are dehydration and dehydroxylation.

Muscovite has dehydroxylation reaction in the temperature range of 820-920 °C. However, the structure of muscovite is very sensitive for powering which results in its dehydroxylation in lower temperatures. When grinded under methanol the crystalline structure is preserved (Földvári, 2001) (Figure 50)

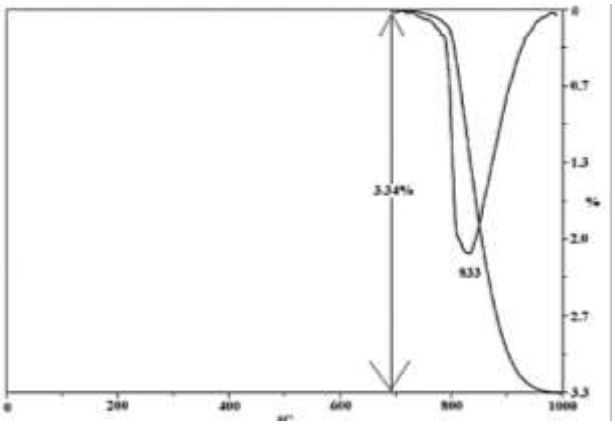

Figure 50- Typical thermo-analytical curve of unpulverised muscovite according to Földvári (2001).

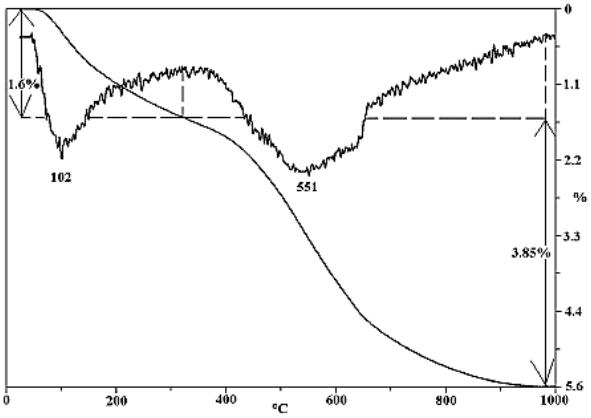

Figure 51- Effects of dry grinding on muscovite according to Földvári (2001).

The dehydroxylation of **kaolinite** occurs between 530-590 °C when it changes by endothermic reaction to meta-kaolinite. Stoichiometric factor of the reaction is 7.17. In addition, between 900-1000 °C there is exothermic reaction accompanying its transformation into crystalline phases (mullite) (Földvári, 2001), (Figure 52).

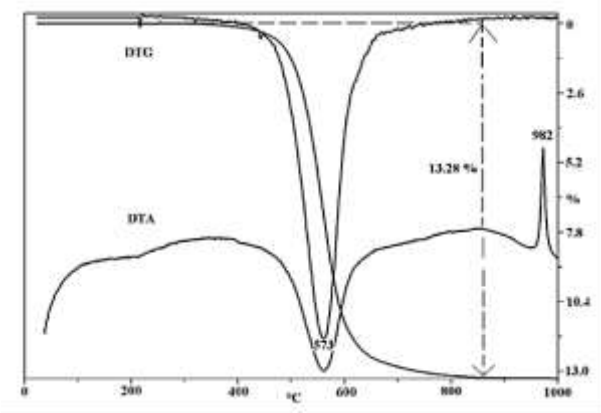

Figure 52- Typical thermo-analytical curve of kaolinite according to Földvári (2001).

The dehydroxylation of the other present phyllosilicates like chlorite and vermiculite can be quite complex. Example of the thermo-analytical curve is presented in Figure 53.

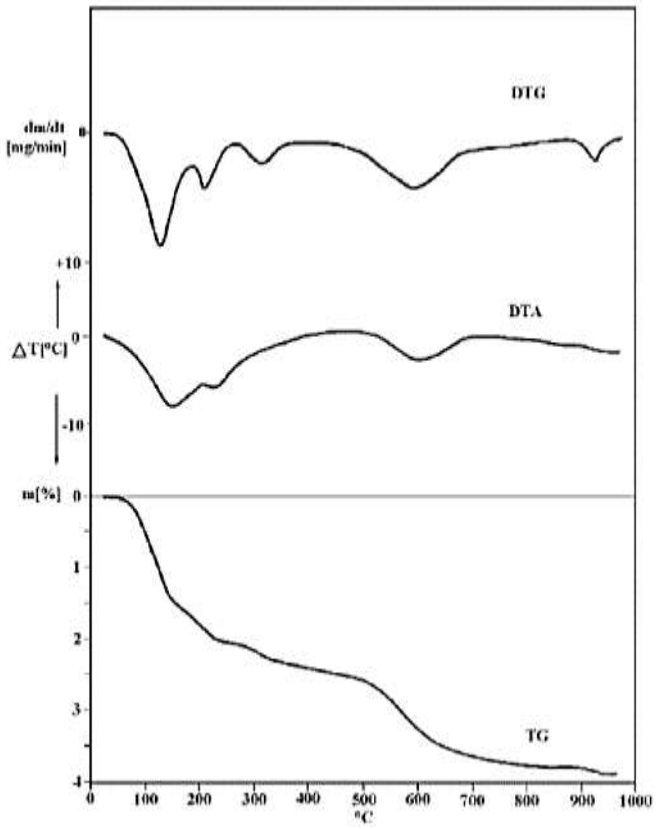

Figure 53- Thermo-analytical curves of interstratified chlorite-vermiculite according to Földvári (2001).

Since from X-ray diffraction results, the presence of muscovite and kaolinite is noted, we can summarize for the ceramic samples the loss of water as shown in Table 19. Since it is a layered system of clays, it was complicated to determine exact reactions up to 200 °C.

Table 19- Cause of loss of water at different temperature ranges.

Cause for loss of water	Temperature range
Physically bound water	0-200 °C
Chemically bound water	200-1050 °C
Muscovite	200-900 °C
Kaolinite	530-590 °C

Loss of water due to muscovite cannot be specifically tracked since there are several other reactions occurring simultaneously.

Thermogravimetric curve comparison

The TG showed a steady loss of mass with temperature for raw clay sample 1. The total loss was about 0.95 %. The loss of physically bound moisture constituted about 2.9 %.

For raw clay sample 2, similar behaviour in loss of mass was deduced from the TG curve Figure 54. The curve was not completely linear for this case. The total loss was noted as 0.78 %.

The overall loss in mass was 0.35 %, lower compared to the previous samples, this aspect was evident in TG curve.

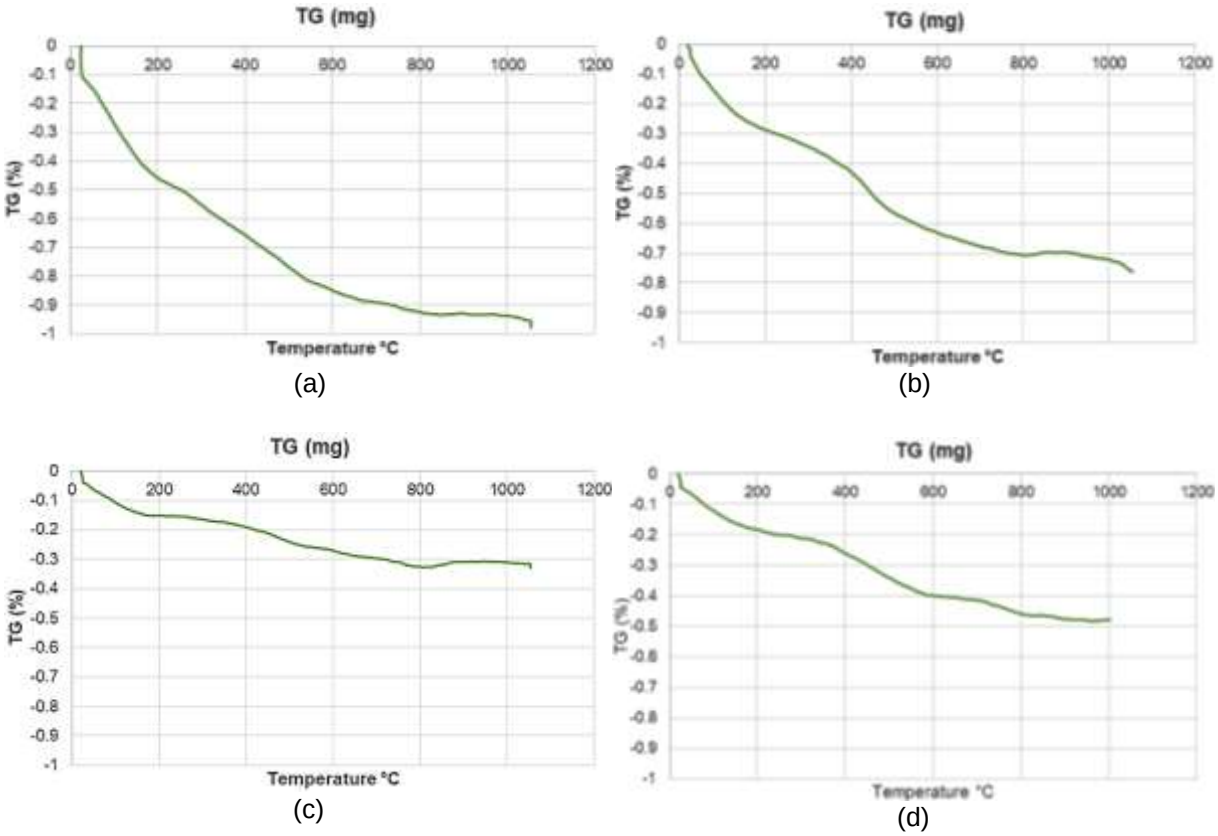

Figure 54- Thermogravimetric curves derived for the four raw clay samples.

Raw clay sample 4 when subjected to thermal analysis gave the indication of presence of kaolinite, initial loss of water. Although the preliminary loss of mass is minor and the reactions are broad between 400-800 °C temperatures. A substantial loss of 1.64 % in mass can be note between temperature ranges of 400-600 °C.

The clay sample 1 showed the most amount loss of about 8 % compared to other clay samples. While the clay samples 3 and 4 showed lower loss of mass. The approximate percentage of loss of mass for all four clay samples is shown below.

Table 20- % of overall loss of mass for all four raw clay samples.

Clay sample	Loss of mass (%)
1	8.025
2	6.255
3	2.795
4	4.376

Clay sample 1 – from "Kamenný rybník"

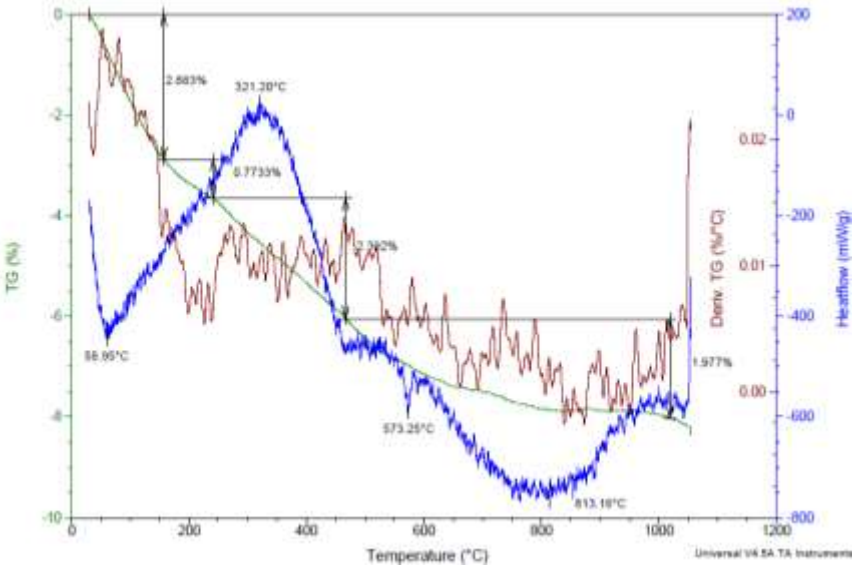

Figure 55- Thermogravimetric, Heatflow and Derivative thermal analysis major highlights for sample 1.

The reaction peak for loss of physically bound moisture was at 58.9 °C. The peak around 300-350 °C signified the loss of water from iron oxides (A. Moropoulou, 1995). Another loss in mass can be noted around 200-450 °C. Kaolinite was recognized by endothermic peak at 573 °C.

Clay sample 2 – from "Cihelna"

An endothermic peak at 70 °C was obtained due to initial water evaporation which lead to 2.13% decrease in mass of sample. Iron oxide liberating water, results in peak at 320 °C. Further the sample showed significant loss in mass with temperature as presented in Figure 55. The peak at 572 °C indicated the presence of kaolinite.

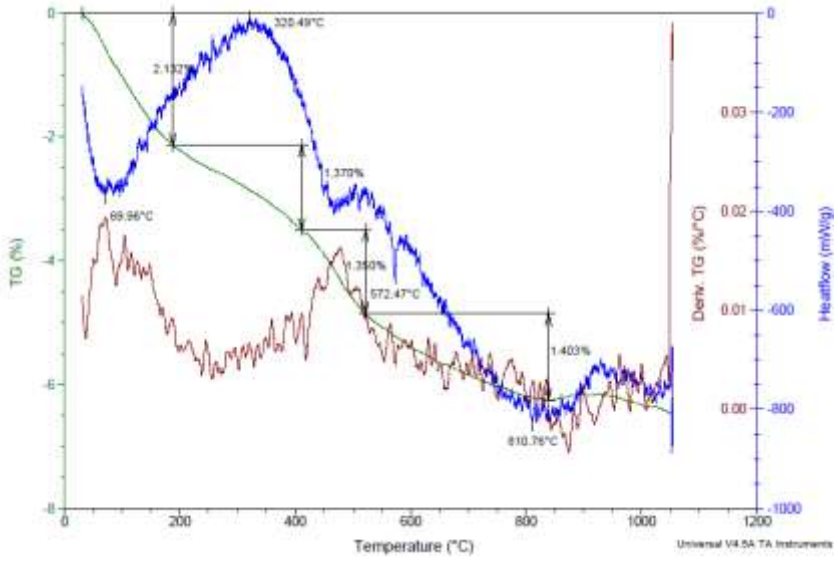

Figure 56- Thermogravimetric, Heatflow and Derivative thermal analysis major highlights for sample 2.

Clay sample 3 – from "Světnov"

The peaks obtained are not prominent and distinct. At 96 °C the first peak due to loss of water was obtained. Broad endothermic and exothermic reactions were observed with temperature in sample 3. Figure 57 presents the comparative graph between TG, DTG and Heatflow for sample 3. The peaks give similar results as sample 1 and 2.

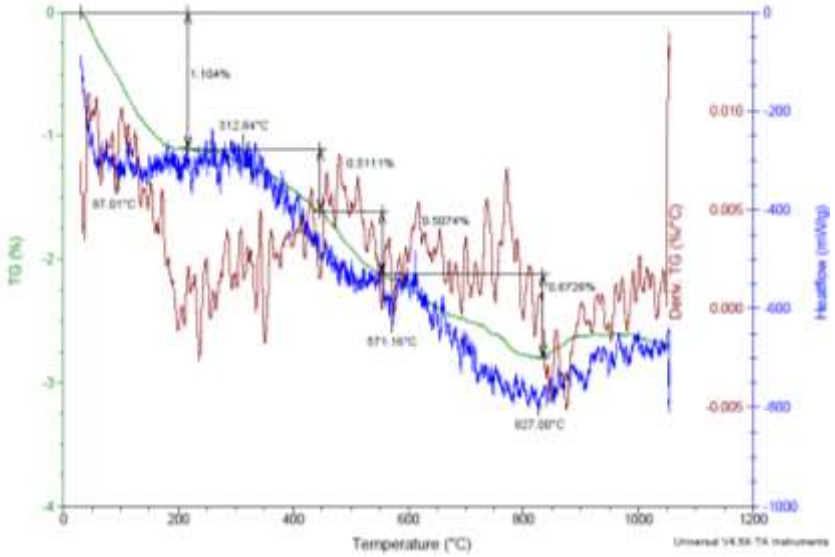

Figure 57- Thermogravimetric, Heatflow and Derivative thermal analysis major highlights for sample 3.

Clay sample 4 – from "Světnov"

Unlike the samples 1, 2 and 3, this sample showed a prominent endothermic reaction at high temperature as presented in Figure 58.

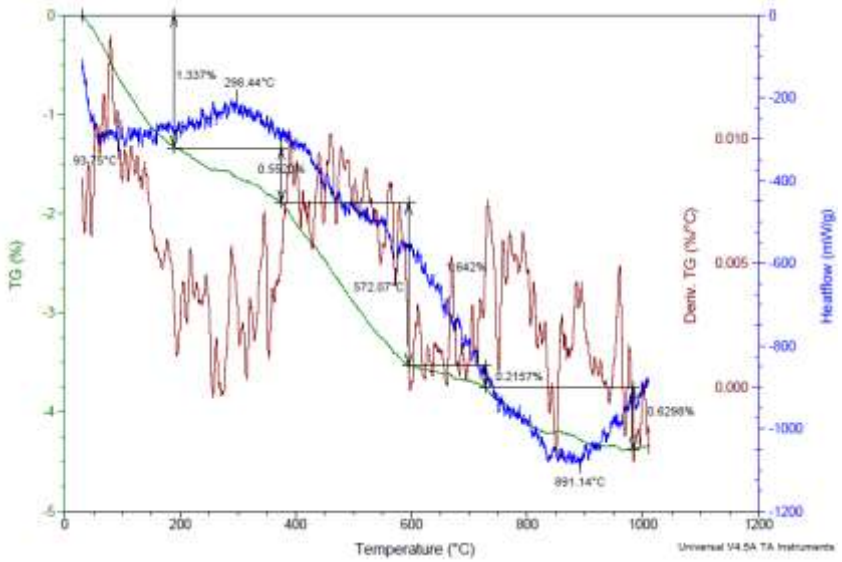

Figure 58- Thermogravimetric, Heatflow and Derivative thermal analysis major highlights for sample 4.

6.5 Optical Microscopy

The composition and microstructure of the burnt and raw ceramic specimens was observed carefully under petrographic microscope. The specimens were assessed for their grain size and occurrence, matrix, pores size and shape.

Description of specimens of clay sample 1:

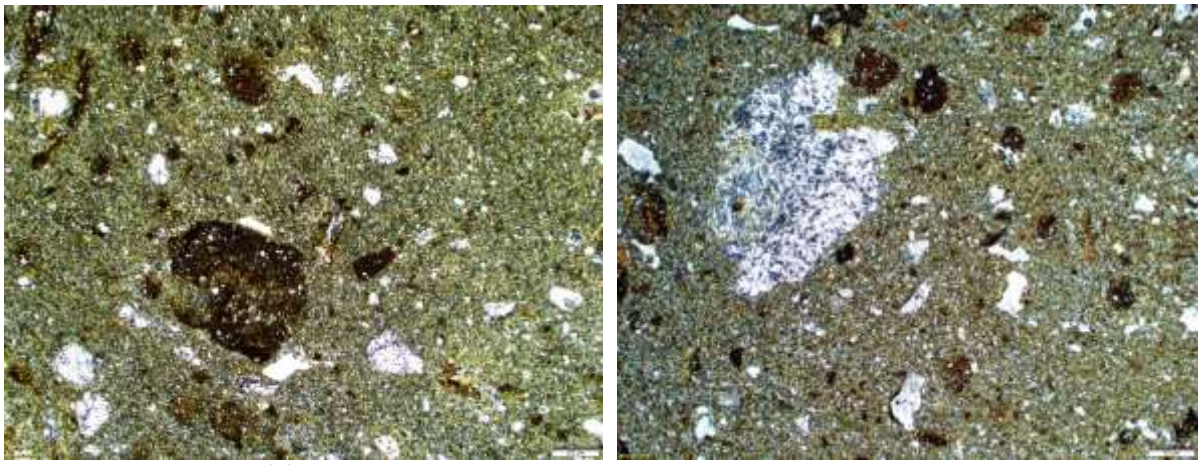

(a) 1-6 (b) 1-1

Figure 59- Optical microscope image in plane polarized light for thin section of specimen 1-6 and 1-1 showing matrix of the specimen with visible grains and pores. View field: 6 mm across.

The raw clay 1-6 thin section was light grey in colour and the observations revealed presence of clay minerals like Quartz and Feldspar in abundance. The specimen had less voids and the matrix was well homogenized with few flat pores observed near the surface. The images were obtained using 1.25x magnification.

The specimen 1-1 showed a well compacted and homogenized matrix with quartz-feldspar grains in majority. Quartz crystals were equant sub-angular in shape and few bigger than 2 mm. The voids observed were rounded and vesicles with the maximum pore size being 1.5 mm. No flat pores were visible near the surface of the specimen (Figure 59).

The specimens 1-2, 1-3 showed a poor matrix distribution with about 20% of inclusion and voids as visible in Figure 60. The inclusion termed is used for dark nodes formed of higher optical density compared to the surrounding matrix. Both samples consisted of gaps (ring voids) between grain and matrix. The pores were found in abundance relative to specimen 1-1. These pores were elongated and vugh (little cavity) shaped. The colour of the matrix turned to light brown in comparison with the raw clay.

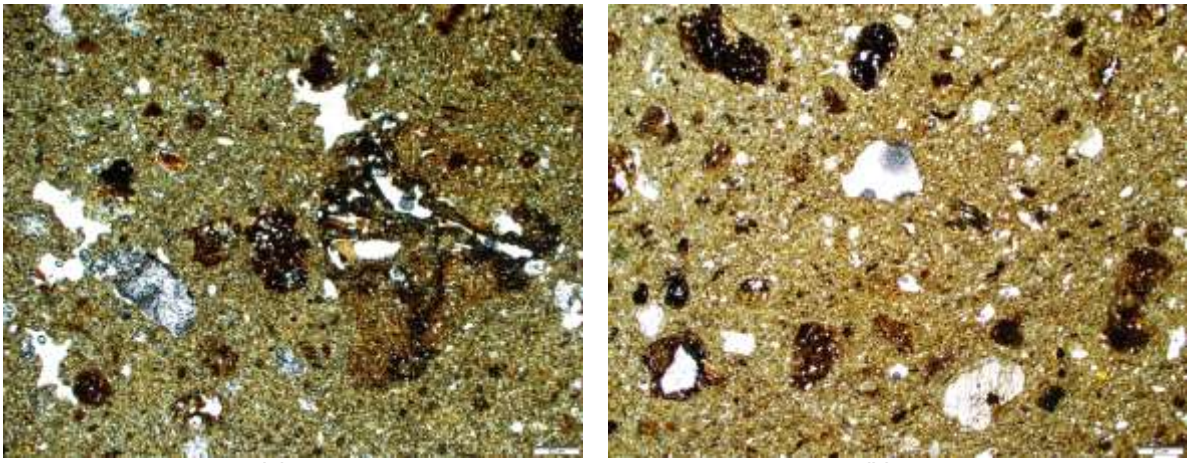

(a) 1-2 (b) 1-3

Figure 60- Optical microscope image in plane polarized light for thin section of specimen 1-2 and 1-3 with prominent pores. View field: 6 mm across.

The specimens 1-4 and 1-5 fired at high temperatures 950 °C and 1050 °C respectively were comparatively darker in shade and the quartz-feldspar grains were less abundant and maximum size around 3-3.5 mm. The matrix had about 20 % voids and the maximum size of these vesicles voids ranged between 1.5-2.3 mm. The specimens exhibited dark nodules with relatively higher optical density than the surrounding matrix (Figure 61).

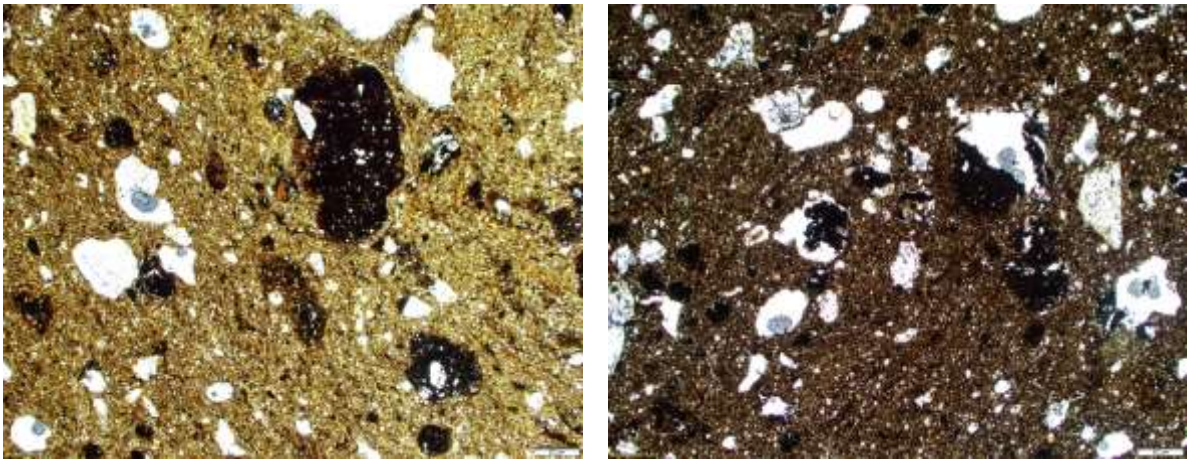

(a) 1-4 (b) 1-5

Figure 61- Optical microscope image in plane polarized light for thin section of specimen 1-4 and 1-5 with prominent pores and dark nodules. View field: 6 mm across.

The matrix consisted of gap surrounding the grains. The quartz-feldspar crystal showed clear to diffuse boundaries.

Description of sample 2 specimens

The raw clay specimen 2-6 was rich in clay minerals and mica as presented in Figure 62. The matrix of this specimen was not homogenised. The presence of quartz-feldspar was observed in abundance with maximum size of 5 mm. Few pores were observed to be of about 2.5 mm in size.

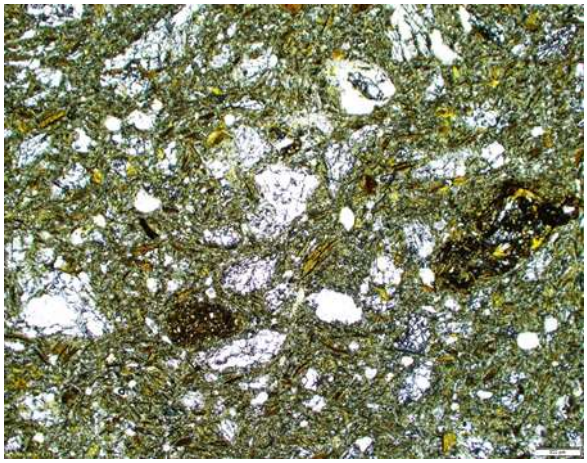

Figure 62- Optical microscope image in plane polarized light for thin section of specimen 2-6. View field: 6 mm across

The specimen 2-1 shows numerous cracks and elongated voids. This specimen had cracked after firing and it was visible in the microscopy too. The specimen even had flat pores near surface and the voids within the specimen had the maximum size of about 5 mm, presented in Figure 63 (b) with 2.5x magnification.

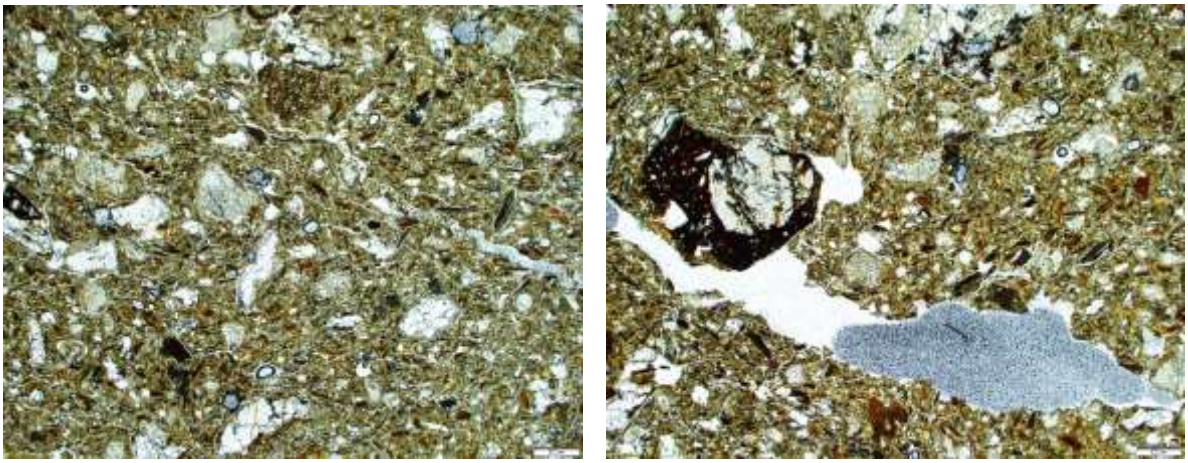

(a) 2-1 (b)

Figure 63- Optical microscope image in plane polarized light for thin section of specimen 2-1; (a) Cracked matrix of the specimen with visible grains and pores; (b) Huge pores within specimen viewed under 2.5x magnification. View field: 2 mm across.

The bubbles in the voids were result of air trapping in the optical adhesive which was used to fix coverslip with thin section. This sample preparation defect was present in specimens 2-2, 2-3, 2-4 and 2-5.

The optical microscope images of specimen 2-2, 2-3, 2-4 and 2-5 are presented in Figure 64. The presence of hematite was found in higher temperature specimen but not very prominent. The specimens become darker in shade as temperature rises above 750 °C. All four specimens showed cracks and voids in the matrix. The shape of crystal grains was observed to be angular, sub-angular and elongated angular. The specimen 2-4 also exhibits dark nodules which were generally result of clay rich spots. The maximum grain sizes measured were 3-4 mm. The diffused boundaries of the grains of quartz and

feldspar were noted. The alteration of mica resulted in elongated black grains in specimens 2-4 and 2-5. The inclusion and voids were estimated to about 40% of the matrix for all four specimens.

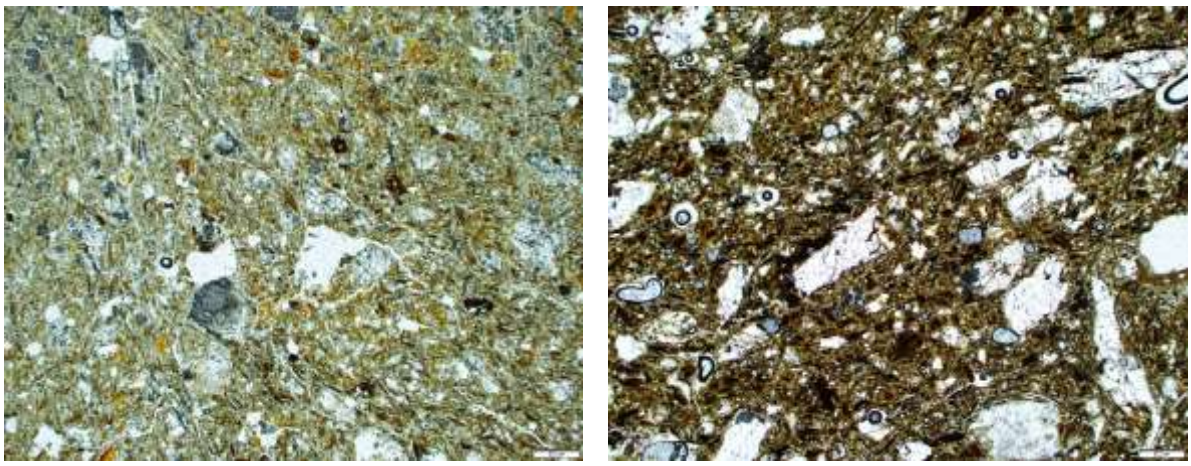

(a) 2-2 (b) 2-3

Figure 64- Optical microscope image in plane polarized light for thin section of specimen 2-2 and 2-3 with visible cracks and small air bubbles trapped in the voids. View field: 6 mm across.

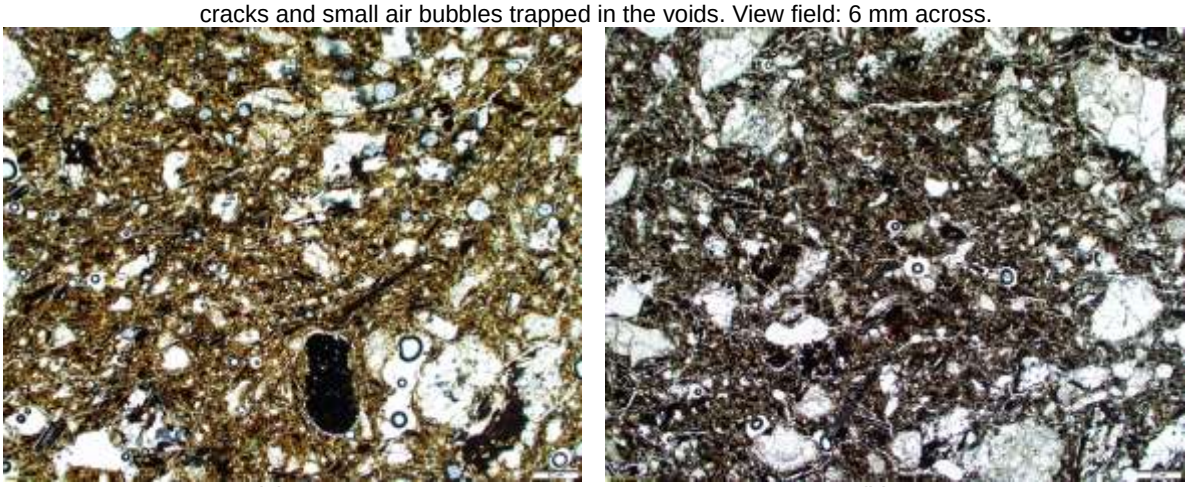

(a) 2-4 (b) 2-5

Figure 65-- Optical microscope image in plane polarized light for thin section of specimen 2-4 and 2-5 with visible cracks and small air bubbles trapped in the voids. View filed: 6 mm across.

Description of sample 3 specimens

For the raw clay specimen 3-6, the inclusion abundance was noted about 10% of the matrix. The matrix was well homogenised and compacted. No flat pores were observed near surface. The maximum grain size was measured as 10 mm. There were few gaps observed between filler and matrix but the number and size of pores in the specimen were less. Dark clay rich inclusions and presence of mica were noted. For the specimen 3-1, maximum grain size measured was 0.8 mm. The matrix of this specimen was well homogenised and there was no gap between filler and matrix. The grains were angular, sub-angular and rounded in shape possessing sharp boundaries. The specimen 3-1 showed few air trapped in the voids formed as sample preparation defect. The optical microscope image of specimen 3-2 and 3-3 are presented below. The specimens showed about 10% of inclusions and voids. Very few elongated voids were observed. The maximum grain size ranged between 2-2.5 mm. The boundaries of the grains were

clear. Specimen matrix was rich in quartz-feldspar. For specimen 3-2, cross polarized light was used to determine the difference between grains and pore as shown in Figure 67.

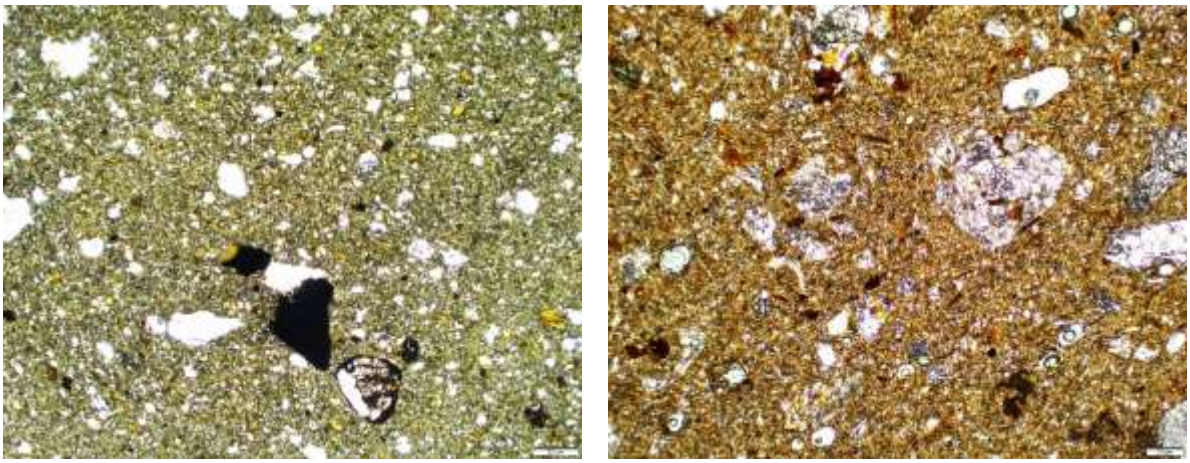

(a) 3-6 (b) 3-1

Figure 66- Optical microscope image in plane polarized light for thin section of specimen 2-2 and 2-3 with visible cracks and small air bubbles trapped in the voids. View field: 6 mm across.

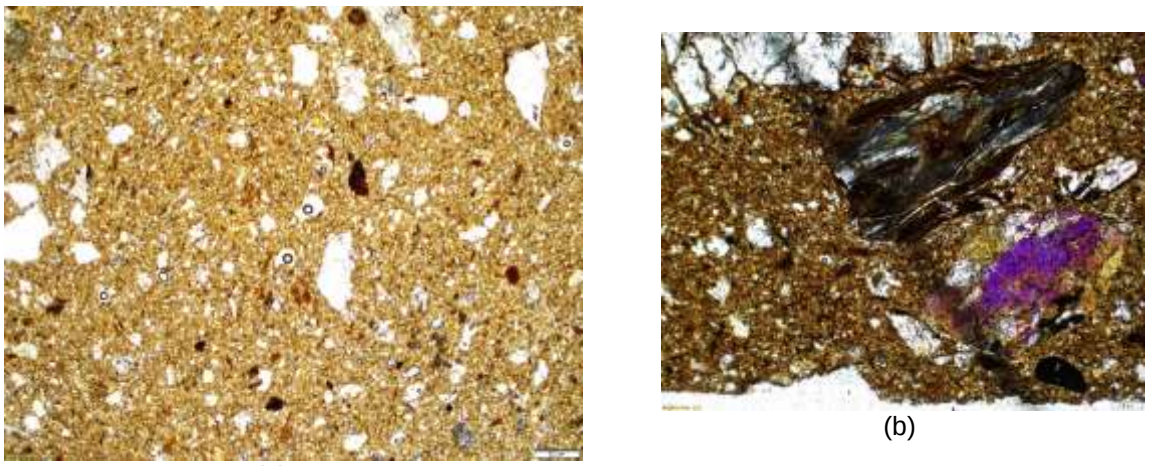

(a) 3-2 (b)

Figure 67- Optical microscope image of thin section of specimen 3-2; (a) In plane polarized light under 1.25x magnification; View field: 6 mm; (b) In cross-polarized light under 2.5x magnification; View field: 2 mm across

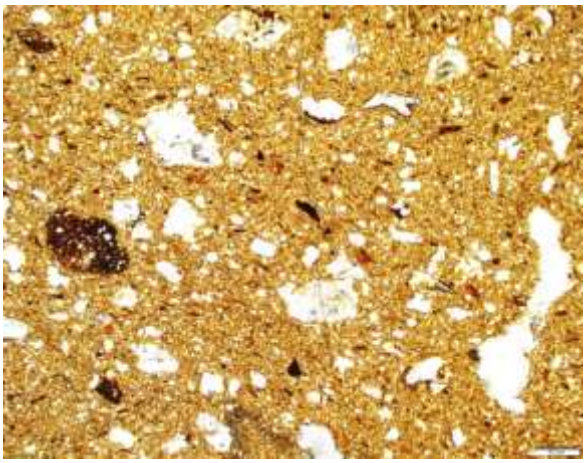

Figure 68- Optical microscope image in plane polarized light for specimen 3-3. View field: 6 mm across.

The specimen 3-3 showed the altered mica split along its planes due to rise in firing temperature. The maximum size of pore measured was about 0.8 mm. The matrix had angular grains with clear boundary. The specimens 3-4 and 3-5 showed darker shade and smaller diffused grains.

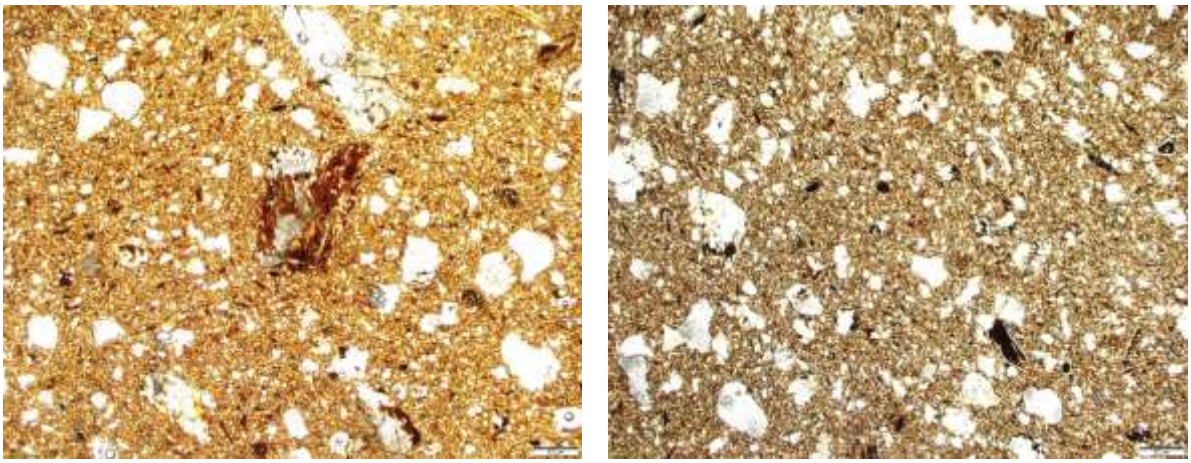

(a) 3-4 (b) 3-5

Figure 69- Optical microscope image in plane polarized light of thin section of specimens 3-4 and 3-5. View field: 6 mm across.

The boundaries of quartz and feldspar in some spots were melted due to high firing temperature. The inclusions and voids constituted about 20% of the matrix. The presence of altered mica was seen throughout the specimen. The maximum grain size for these specimens ranged between 3-4 mm. Elongated voids and cracks were found in 3-5 specimen as shown in Figure 70.

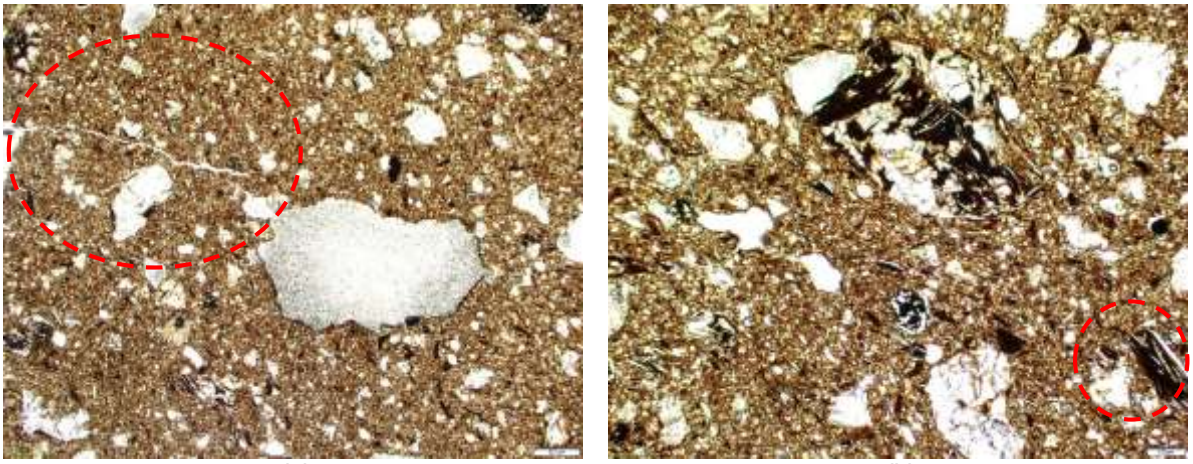

(a) (b)

Figure 70- Optical microscope image of thin section of specimen 3-5; (a) Cracks and pores observed under 1.25x magnification; View filed: 6 mm across; (b) Altered mica observed under 2.5x magnification. View field: 2 mm across.

Description of sample 4 specimens

The raw clay specimen 4-6 was homogenized with maximum grain size measured as 4 mm. The pores were rounded with bubbles. The grains showed well defined and distinct boundaries. For the specimens 4-1 and 4-2, the inclusions and voids constituted 20-40% of the matrix. Elongated and channelled pores were evident and abundant.

Moreover clay rich inclusions surrounded by ring voids were observed in both the specimens (Figure 71). The maximum grain size (Quartz grain) was measured to be 6 mm.

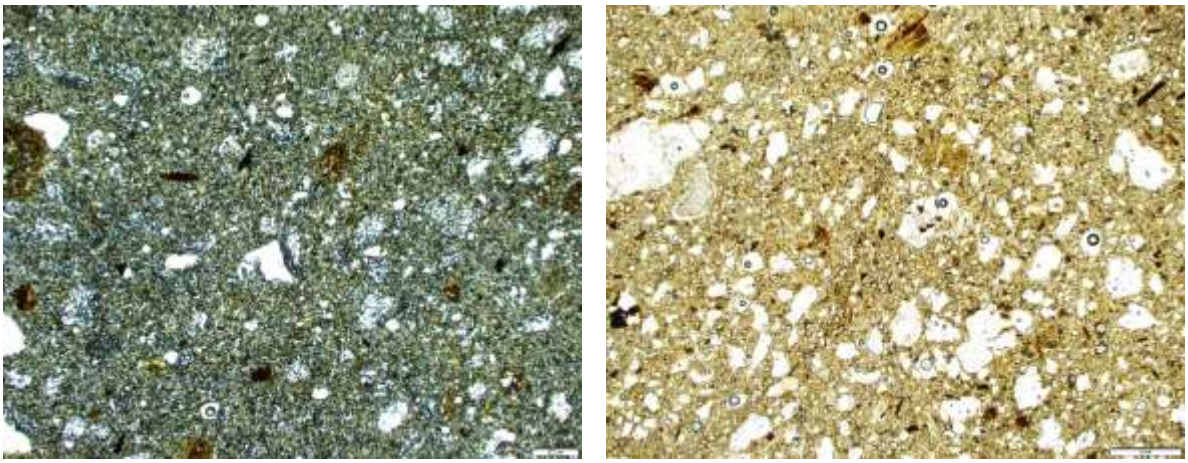

(a) 4-6 (b) 4-1

Figure 71- Optical microscope image in plane polarized light of thin section of specimens 4-6 and 4-1 showing the matrix with pores and grain distribution. View field: 6 mm across.

The specimens 4-3 and 4-4 showed darker core which may have been caused due to insufficient penetration of oxygen during the firing process (Quinn, 2013). Due to loss of water and drying few cracks were observed in these specimens. The ring voids can be seen in Figure 73.

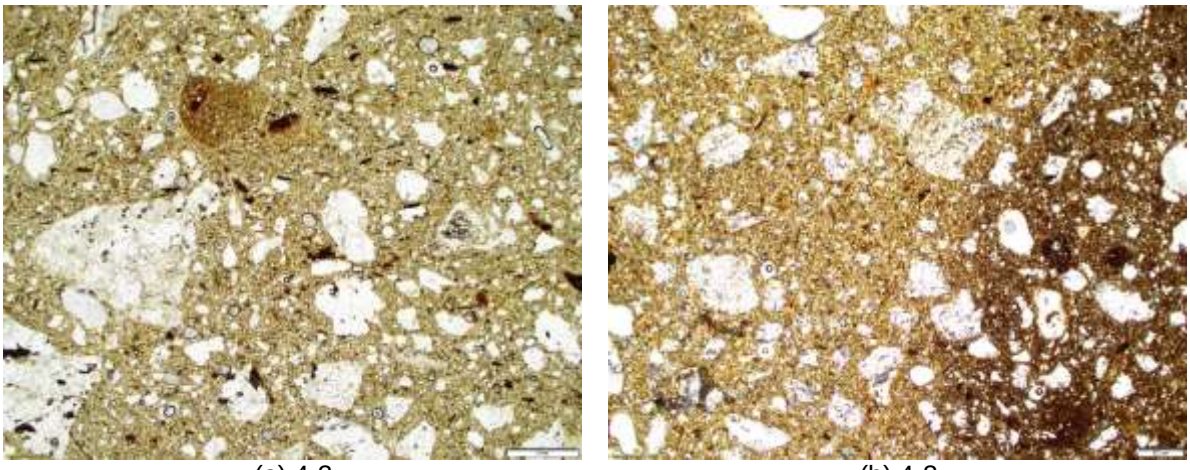

(a) 4-2 (b) 4-3

Figure 72- Optical microscope image in plane polarized light of thin section of specimens 4-2 and 4-3; (a) Large quartz grain and filler gap in specimen 4-2; (b) Darker core observed in specimen 4-3. View field: 6 mm across.

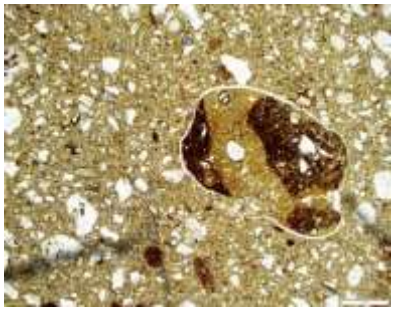

Figure 73- Optical microscope image in plane polarized light showing the ring void under 2.5x zoom for specimen 4-2. View field: 0.15 mm across.

The dark core vanishes in specimen 4-5 which was burnt at the highest temperature. The specimen 4-5 showed well distributed grains and pores in the matrix however these inclusions constituted about 40% of the matrix. Very distinct ring voids were seen around the quartz grains. This can be due to melting of the grains, thus creating voids surrounding it.

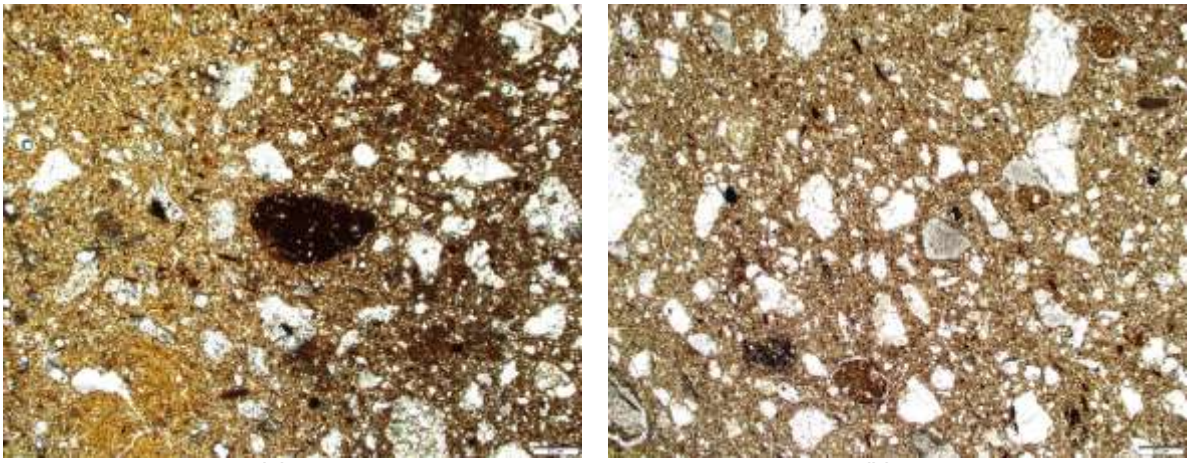

(a) 4-4 (b) 4-5

Figure 74- Optical microscope image in plane polarized light of thin section of specimens 4-4 and 4-5; (a) Darker core observed in specimen 4-4; (b) Matrix with visible grains and pores in specimen 4-5. View field: 6 mm across.

Description of original tile

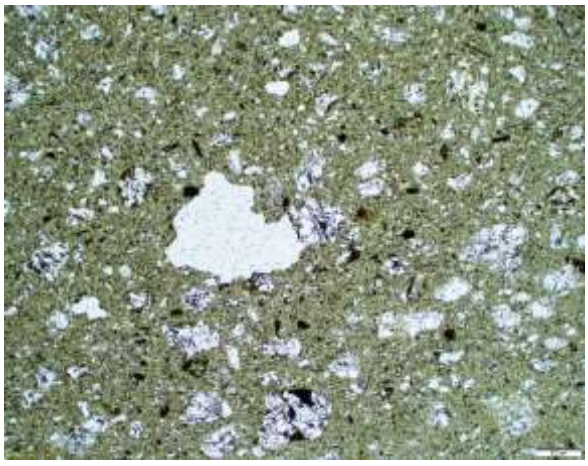

Figure 75- Optical microscope image in plane polarized light of thin section of the original tile. View field: 6 mm across.

The observations made for the original tile showed a well compacted and homogenized matrix of the specimen. The maximum grain size recorded was 3 mm. There were no prominent cracks but few air bubbles trapped in pores. The matrix constituted of 10 % inclusions and pores. Quartz and feldspar were dominant in this matrix. Dark inclusions were scarcely observed. The general matrix contained of almost similar sized grains. The observations indicated a well compacted specimen.

7. DISCUSSION

The general estimation of the burning temperature of the old brick can be made using the results from X-ray diffraction. Since there was no presence of hematite detected for the original brick, the burning temperatures 950 °C and 1050 °C were less probable. The original tile showed presence of muscovite with 1.7 wt.%. Muscovite decomposes at high temperatures thus the highest temperature of 1050 °C can be eliminated for this tile. There was no presence of kaolinite in the mineralogy of the original tile suggesting that the lower temperatures (<650°C) can be considered less creditable. Moreover the Figure 76 compares the content of specimens burnt at 850 °C i.e. 1-3, 3-3 and 4-3 with the original tile. Specimens of sample were not considered as they do not have muscovite content.

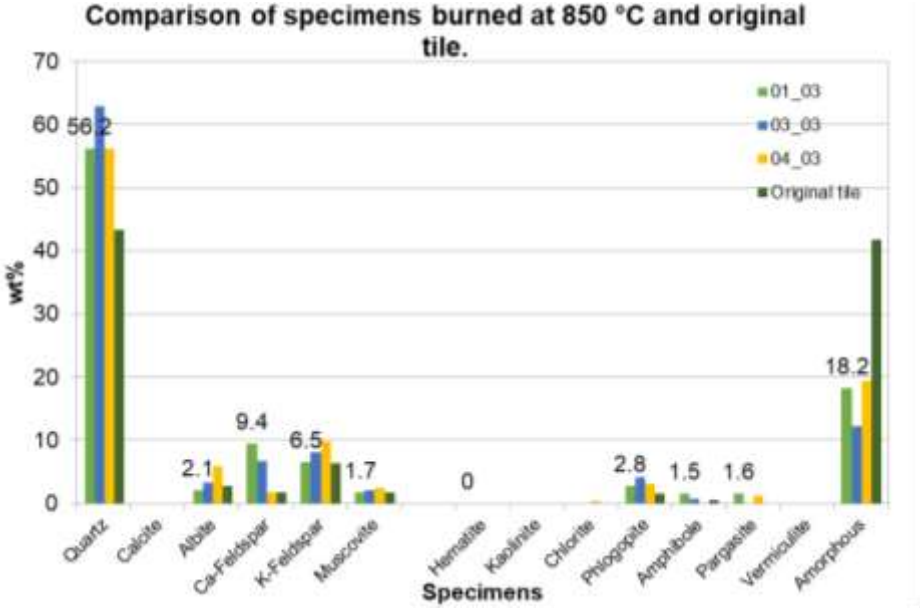

Figure 76- Mineralogy of specimens burnt at 850 °C and the original tile.

The other specimen possessing similar mineralogical contents was specimen 3-2 of burnt at 750 °C.

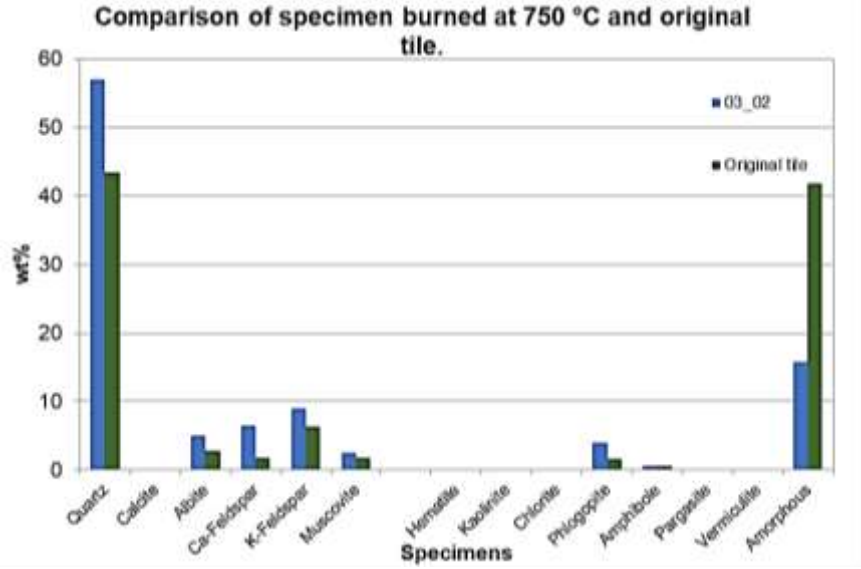

Figure 77- Mineralogy of specimen 3-3 burnt at 750 °C and the original tile.

The amorphous content of the original tile is too high in comparison with the prepared specimens. Alberto Viani (2016) states that the feldspar are less useful as indicators of firing temperature since they get involved in reactions at high temperature or may form after form after phyllosilicates decomposition. Thus the variations obtained for feldspar content may not be the best form to determine the burning temperature.

For the characterization of the burnt specimens the outcomes from XRD, thermal analysis, mechanical tests and optical microscopy can be discussed and correlate for better understanding of behaviour.

The results from the thermal analysis of raw clay of the four samples were correlated with the burnt specimens. The observations confirmed that the dehydroxylation of muscovite occurs in range of 200-950 °C leading to loss in its content. The comparison of the mineralogy of the four raw clays is provided in Table 21.The clay samples 1, 3 and 4 had alike mineralogy and content while clay sample 2 contained less amount of quartz and more amount of feldspar.

Table 21- Mineralogy of the four raw clays.

Phase	**1**	**2**	**3**	**4**
Quartz	64	54,6	64,2	62,9
Albite	6	9,5	8,4	7,5
Ca-feldspar	2,3	9,4	2,1	1,6
K-Feldspar	9,1	7,5	8,1	12,4
Muscovite	3,5	6,9	5,7	4,4
Kaolinite	5,3	4,1	4,3	4,9
Chlorite	1,7	0,3	1,1	1,2
Vermiculite	6	4,4	4,3	3,4
Amphibole	1,6	1,9	0,9	0,9
Pargasite	0,5	1,4	1	1

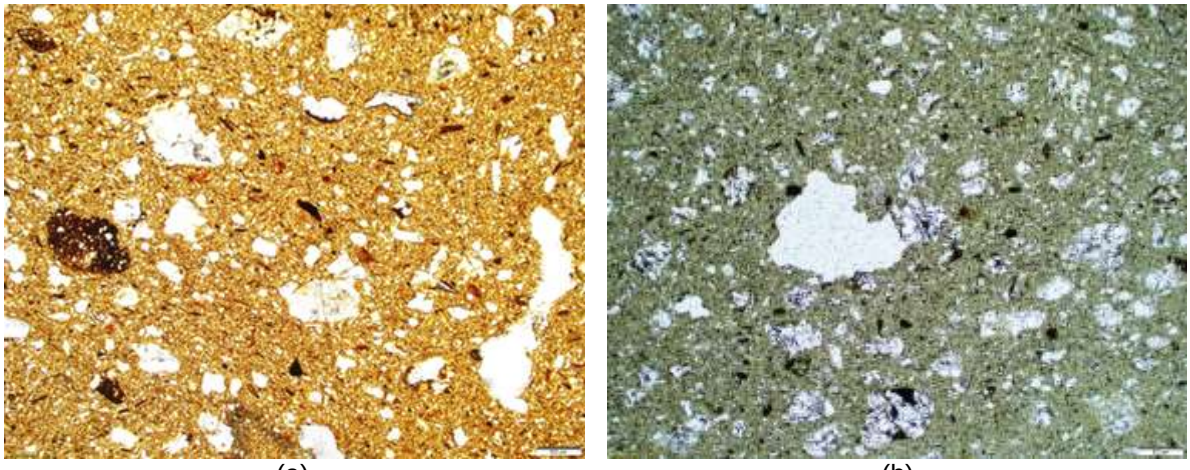

(a) (b)

Figure 78- Comparison of optical microscopy image in plane polarized light for; (a) Specimen 3-3; (b) The original tile; View field: 6 mm across

The microstructure of all the specimens was observed carefully under petrographic microscope contributing to the confirmation of decreased quartz and feldspar crystals, increase in amorphous with increase in temperature. The optical images of original tile with the specimen 3-3 can be seen in Figure 78. The matrix of both the specimens were similar but the original tile showed fewer pores compared to specimen 3-3. Nevertheless this may be caused in specimen 3-3 due insufficient compaction.

The open pores were noted to be low for specimens burnt at high temperatures but the microscopic observations showed vugh and vesicle pores. The cause behind these results were assumed to be the closed pore content and this assumption was confirmed from the results of degree of pore interconnectivity. However the compressive strength achieved was substantially high for the specimens burnt at 1050 °C. Thus the open porosity had direct influence on the compressive strength of the specimens.

The four clay sample tested were not the most representative samples based on their collection conditions, hence the resulting values and observations cannot be generalized for the entire province.

8. CONCLUSION

The study provided substantial information about the behaviour of local clay burnt at different temperatures. The clay samples were collected in 5 km radius of vicinity from the church. The data of the tests results of the compressive strength and porosity performed on the representative specimens, indicated that specimens burnt at 1050°C possessed low porosity in range of 29-33% and higher compressive strength up to 20 MPa. At the same time their degree of interconnectivity was high in range of 23-26%, this indicated presence of closed pores within the specimens. The mineralogy cannot be directly related to strength, since strength is one of the functions of mineralogy along with internal changes, microstructure and pore connectivity. The X-ray diffraction results stated that clay sample 2 obtained from Cihelna was different in terms of mineralogy compared to the other three clays collected from Světnov andKamenný rybník. The mineralogy consisted of mainly quartz and feldspar followed by albite. Apart from these a group of phyllosilicates minerals was detected and no presence of calcite was recorded. The collected clay samples showed certain regional mineralogical similarities but their sampling position was superficial. They representativeness in terms of quality of raw material for production burnt clay units was therefore limited. This was confirmed when the sample 2 was destroyed during the burning.

However, the experimental work provided information about the behaviour of the local clays when burnt at different temperatures that could be compared with the historic tiles.

The results of X-ray diffraction carried out on the original tile indicated clay as the raw material with mineralogy comparable with the experimental specimens burnt at 750 °C and 850 °C. Thus this specific tile from the flooring of the St. John of Nepomuk may be possibly prepared using locally available raw clay. Since the clay pits did exist in 18th and 19th century as evidenced by the data provided in the old cadastral and military maps, one of the selected sites for collection of raw material for this study could had been probable source of raw material for the original tile of the church. Thus the local clays burnt between the temperature range 750-850 °C can be suggested for the reproduction process of the original red coloured tiles. Nevertheless certain observations should be kept in mind before selecting the burning technology. One of them being the core of the tested original tile was darker. This effect possibly was due to less oxygen content or more carbon oxides in the manufacturing conditions. The specific historic production technology was not covered by the experiments should be studied further.

The approach of this experimental study was in right direction for understanding the phase transformations of minerals, the pore structure and interconnectivity, and mechanical behaviour. Though the quantitative results were not exactly matching the original tile, we could manage to estimate the mineralogy and burning temperature. Thus the research methodology and tests can be acknowledged as beneficiary for the characterization of burnt clay units.

9. FUTURE SCOPE

In order to obtain additional results matching closer the original composition, more clay samples can be collected using detailed geological survey data and proper clay probing tools allowing assessment along depth profiles. The specimens prepared from clay samples can be characterized using additional combinations of temperatures with similar laboratory tests. More detailed analysis of the original tiles should be undertake in order to cover all variables, e.g. based on colour differences observable by naked eye. However, this study should be carried out in accordance with the conservation plan as the sampling is invasive and destructive method.

10. REFERENCES

A. Moropoulou, A. B. (1995). Thermal analysis as a method of characterizing ancient ceramic technologies. *Thermochimica Acta 2570*, (pp. 743-753). Italy.

Alberto Viani, K. S. (2016). Assessment of firing conditions in old fired-clay bricks: The contribution of X-ray powder diffraction with the Rietveld method and small angle neutron scattering. *Material Characterization*, 33-43.

Barua, M. R. (2013). Indian Journal of Pure & Applied Physics. *X-ray diffraction and Fourier transformationinfrared spectra of the bricks of the Kamakhya temple*, 745-748.

Berger, M. B. (2010). THE IMPORTANCE AND TESTING OF DENSITY / POROSITY / PERMEABILITY / PORE SIZE FOR REFRACTORIES . *The Southern African Institute of Mining and Metallurgy Refractories*, (pp. 101-116).

Brindley, G. W. (n.d.). STRUCTURAL MINERALOGY OF CLAYS. *Clay and Clay Technology*, 33-43.

Church of St. John of Nepomuk. (2016, 3 21). Retrieved from Hidden Architecture: http://www.hiddenarchitecture.net/2016/03/church-of-st-john-of-nepomuk.html

Dijk, B. v. (2017, March 29). *Vysocina map Gustav Mahler*. Retrieved from Gustav-mahler.eu: https://www.gustav-mahler.eu/index.php/plaatsen/194-czech-republic/vysocina-region/3361-vysocina-map

Fierascu, R.-M. I.-L. (2009). Thermal analysis of Romanian ancient ceramics. *J Therm Anal Calorim (2010)* (pp. 393–398). Budapest: Akade´miai Kiado´.

Földvári, M. (2011). *Handbook of thermogravimetric system of minerals and its use in geological practice.* Budapest: The Geological Institute of Hungary.

Fuxa, F. (n.d.). *Shutterstock*. Retrieved from Shutterstock.

Geoinformation, L. o. (n.d.). *1st Military Survey - Bohemia*. Retrieved from Oldmaps.geolab.cz: http://oldmaps.geolab.cz/map_viewer.pl?&map_root=1vm&map_list=c200&map_region=ce&lang=en

Giuseppe Cultrone, *. E. (2004). Influence of mineralogy and firing temperature on the. *Journal of the European Ceramic Society 24*, 547–564.

Giuseppe Cultrone, *. I. (2005). Mineralogical and physical characterization of the bricks used in the construction of the bTriangul BastionQ, Riga (Latvia). *Applied Clay Science* , 297– 308.

Johnson, R. T. (1940). SOME PROPERTIES OF THE PORE SYSTEM IN BRICKS AND. *National Bureau of Standard, Volume 25*, 712-729.

K Ambrose, M. A. (2001). *Brick Clay: Issues for Planning.* Norwich: The Queen's Printer and Controller of HMSO.

Mojmir Horyna, J. R. (2008). *Kostel sv. Jana Nepomuckého na Zelené hoře.* Národni památkovy ústav.

Quinn, P. S. (2013). *Ceramic Petrography- The interpretation of Archaeological Pottery and related artefacts in thin section.* Oxford: Archaeopress and PatrickSean Quinn .

Ronald Stulz, K. M. (1993). *Appropriate Building Materials- A Catalogue of Potential Solutions.* SKAT, IT Publications and GATE.

Ruth Ann Armitage a, *. L. (2006). Characterization of bricks and tiles from the 17th-century brick Chapel. *Journal of Archaeological Science 33*, 615-627.

Růžička, S. (2014). *Jan Blažej Santini Aichel: A Brief Guide to the Life and Work of a Czech Baroque-gothic Genius.* Video-foto-Kunc.

space, A. o. (2017, 10 5). *THE VYSOČINA REGION WAKES UP*. Retrieved from Art of Space: http://artofspace.cz/kraj-vysocina-se-probouzi/

Stabilní katastr Čech - Světnov, původně Swietnow. (n.d.). Retrieved from Archivnimapy.cuzk.cz: http://archivnimapy.cuzk.cz/cio/data/main/cio_query_01.html?mapno_cm=c7622-1

ThermoARL. (1999). *Basics of X-ray diffraction.* Switzerland: ThermoARL- CH publication.

UNESCO. (1994). *World Heritage Convention*. Retrieved from whc.unesco.org: http://whc.unesco.org/en/statesparties/cz/documents/

Zamekzdar. (n.d.). *Zelena Hora*. Retrieved from In-Pocasi: https://leto.in-pocasi.cz/zelena-hora/